University of Groningen

A fetal wave of human type 3 effector gamma delta cells with restricted TCR diversity persists into adulthood

Tan, Likai; Fichtner, Alina Suzann; Bruni, Elena; Odak, Ivan; Sandrock, Inga; Bubke, Anja; Borchers, Alina; Schultze-Florey, Christian; Koenecke, Christian; Foerster, Reinhold

IMPORTANT NOTE: You are advised to consult the publisher's version (publisher's PDF) if you wish to cite from it. Please check the document version below.

Document Version
Publisher's PDF, also known as Version of record

[Link to publication in University of Groningen/UMCG research database](#)

T CELLS

A fetal wave of human type 3 effector γδ cells with restricted TCR diversity persists into adulthood

Likai Tan[1,2†], Alina Suzann Fichtner[1†], Elena Bruni[1], Ivan Odak[1], Inga Sandrock[1], Anja Bubke[1],
Alina Borchers[3], Christian Schultze-Florey[1,4], Christian Koenecke[1,4], Reinhold Förster[1,5],
Michael Jarek[6], Constantin von Kaisenberg[7], Ansgar Schulz[8], Xiaojing Chu[9,10], Bowen Zhang[10],
Yang Li[5,10], Ulf Panzer[3], Christian F. Krebs[3], Sarina Ravens[1,5‡], Immo Prinz[1,2,5‡*]

Accumulating evidence suggests that the mouse embryonic thymus produces distinct waves of innate effector γδ T cells. However, it is unclear whether this process occurs similarly in humans and whether it comprises a dedicated subset of innate-like type 3 effector γδ T cells. Here, we present a protocol for high-throughput sequencing of *TRG* and *TRD* pairs that comprise the clonal γδTCR. In combination with single-cell RNA sequencing, multiparameter flow cytometry, and TCR sequencing, we reveal a high heterogeneity of γδ T cells sorted from neonatal and adult blood that correlated with TCR usage. Immature γδ T cell clusters displayed mixed and diverse TCRs, but effector cell types segregated according to the expression of either highly expanded individual Vδ1⁺ TCRs or moderately expanded semi-invariant Vγ9Vδ2⁺ TCRs. The Vγ9Vδ2⁺ T cells shared expression of genes that mark innate-like T cells, including *ZBTB16* (encoding PLZF), *KLRB1*, and *KLRC1*, but consisted of distinct clusters with unrelated Vγ9Vδ2⁺ TCR clones characterized either by *TBX21*, *FCGR3A*, and cytotoxicity-associated gene expression (type 1) or by *CCR6*, *RORC*, *IL23R*, and *DPP4* expression (type 3). Effector γδ T cells with type 1 and type 3 innate T cell signatures were detected in a public dataset of early embryonic thymus organogenesis. Together, this study suggests that functionally distinct waves of human innate-like effector γδ T cells with semi-invariant Vγ9Vδ2⁺ TCR develop in the early fetal thymus and persist into adulthood.

INTRODUCTION

γδ T cells are an evolutionarily conserved subset of T lymphocytes that can respond to microbial stimuli and provide tissue surveillance independent of major histocompatibility complex–peptide recognition. Because of their seemingly intrinsic cytotoxicity toward a large array of tumors, γδ T cells are the subject of current efforts to design anticancer immunotherapies (*1*). Although generally regarded as innate-like T cells, γδ T cells display a great level of phenotypic heterogeneity (*2*). The most abundant γδ T lymphocytes in human adult blood are defined by a semi-invariant T cell receptor (TCR) composed of a TCRγ chain (*TRG*) using the variable (V) segment Vγ9 (*TRGV9*) rearranged to the joining (J) segment JP (*TRGJP*) and a TCRδ chain (*TRD*) using a Vδ2 segment (*3*). Such Vγ9Vδ2⁺ T cells display a considerable TCR diversity but respond to microbial and tumor-derived metabolites called phosphoantigens (*4*), which are associated with and influence the conformation of butyrophilin

molecules BTN3A1 (*5*) and BTN2A1 (*6*, *7*). Because of their human leukocyte antigen (HLA)–independent mode of action, Vγ9Vδ2⁺ T cells can be considered for allogeneic clinical applications such as antitumor immunotherapy (*8*). Furthermore, Vγ9Vδ2⁺ T cells share common features with other human innate-like T cells, including invariant natural killer T (NKT) and mucosa-associated invariant T (MAIT) cells that express PLZF (*9*, *10*). The remaining non-Vγ9Vδ2⁺ human γδ T cell subsets express diverse *TRG* rearrangements and preferentially pair with Vδ1 (*3*). Information about specific ligands binding to those Vδ1⁺ TCRs is still fragmentary; however, recent findings showed expansion of individual Vδ1⁺ clones in response to environmental antigens such as viral stimuli (*11*, *12*).

The correlation of γδTCR usage, TCR-specific activation, and acquisition of γδ T cell effector function is of great interest. In mice, distinct waves of effector γδ T cells with restricted TCR diversity develop sequentially in the fetal thymus (*13*). In particular, interleukin-17 (IL-17)–producing effector γδ T (γδT17) cells with a type 3 immune signature are exclusively generated before birth and persist throughout the entire life as self-renewing, tissue-resident T cells in a diverse range of tissues (*14*, *15*). There are parallels in humans, as Vγ9Vδ2⁺ T cells with restricted TCR diversity are preferentially generated before birth, expand postnatally, and persist into adulthood (*16–19*). However, whether and to which extent human γδ T cells already acquire effector function in the thymus are a matter of debate. Postnatal thymi contained γδ T cells with immense TCR diversity (*20*), but these were not found to be equipped with effector functions such as interferon-γ (IFN-γ) or IL-17 production (*21*). In contrast, recent data suggested that the human fetal thymus does generate invariant non-Vγ9Vδ2⁺ effector γδ T cells that express invariant germline-encoded CDR3γ and CDR3δ repertoires (*22*). Furthermore, a recent study compared human Vδ1⁺ and Vδ2⁺ γδ T cells by single-cell RNA sequencing (scRNA-seq) and concluded that

[1]Institute of Immunology, Hannover Medical School (MHH), Hannover, Germany. [2]Institute of Systems Immunology, Hamburg Center for Translational Immunology (HCTI), University Medical Center Hamburg-Eppendorf, Hamburg, Germany. [3]Translational Immunology, III. Department of Medicine, Hamburg Center for Translational Immunology (HCTI), University Medical Center Hamburg-Eppendorf, Hamburg, Germany. [4]Department of Hematology, Hemostasis, Oncology, and Stem Cell Transplantation, Hannover Medical School, Hannover, Germany. [5]Cluster of Excellence RESIST (EXC 2155), Hannover Medical School, Hannover, Germany. [6]Genome Analytics, Helmholtz Centre for Infection Research, Braunschweig, Germany. [7]Department of Obstetrics, Gynecology, and Reproductive Medicine, Hannover Medical School, Hannover, Germany. [8]Department of Pediatrics, University Medical Center Ulm, Ulm, Germany. [9]Department of Genetics, University of Groningen, University Medical Center Groningen, Groningen, Netherlands. [10]Department of Computational Biology for Individualised Medicine TWINCORE, Helmholtz Centre for Infection Research and Hannover Medical School, Hannover, Germany.
*Corresponding author. Email: i.prinz@uke.de
†These authors contributed equally to this work.
‡These authors contributed equally to this work.

both displayed parallel maturation trajectories, starting with expression of maturation-defining genes including *CCR7*, *IL7R*, and *CD27* and gradually acquiring cytotoxicity-related genes such as *NKG7*, *PRF1*, and *FCGR3A* (*23*).

To directly assess the role of the TCR in guiding the activation and differentiation of individual Vγ9Vδ2+ and non-Vγ9Vδ2+ γδ T cell clones, we sorted total γδ T cells from cord (CB) and adult peripheral blood (PB) and combined scRNA-seq with single-cell sequencing of paired *TRG* and *TRD* rearrangements (scTCR-seq). We established a minimal flow cytometric panel comprising three TCR-specific and nine surface markers that reproduces the phenotypic map of human γδ T cell subsets obtained by scRNA-seq. We found functional heterogeneity of immature and differentiated γδ T cells, which segregated according to γδTCR usage and effector phenotype. We identified distinct type 1– and type 3–like subsets of Vγ9Vδ2+ T cells that used distinct sets of TCR clonotypes. In addition, γδ T cells with a type 3 immunity signature were already present in neonatal CB and in early fetal thymus from weeks 8 and 9, which supports the hypothesis that these cells might be generated in an early fetal wave.

RESULTS

scRNA-seq reveals high heterogeneity among human γδ T cells

To investigate transcriptional programs of human γδ T cells at birth and in adulthood, total γδ T cells were isolated from two unrelated neonatal CB samples (CB_donor1 and CB_donor2) and two unrelated adult PB samples (PB_donor1 and PB_donor2) via flow cytometric sorting for scRNA-seq (fig. S1). After quality control, a total of 25,904 γδ T cells from all respective donors (median gene number = 1434; median UMI (unique molecular identifier) = 3964) were considered for post-analysis (fig. S2A). On the basis of transcriptomic profiles, these γδ T cells were projected by Uniform Manifold Approximation and Projection (UMAP), and unsupervised clustering with adjustment by differential gene expression analysis among neighboring clusters identified 12 cell clusters (c1 to c12) (Fig. 1A). A polarized age-dependent distribution was observed

(Fig. 1B). Neonatal γδ T cells dominated clusters c1 to c5, whereas clusters c6, c7, c9, and c12 were more heterogeneous. Adult γδ T cells formed most of c8, c10, and c11 (Fig. 1, B and C). A total of
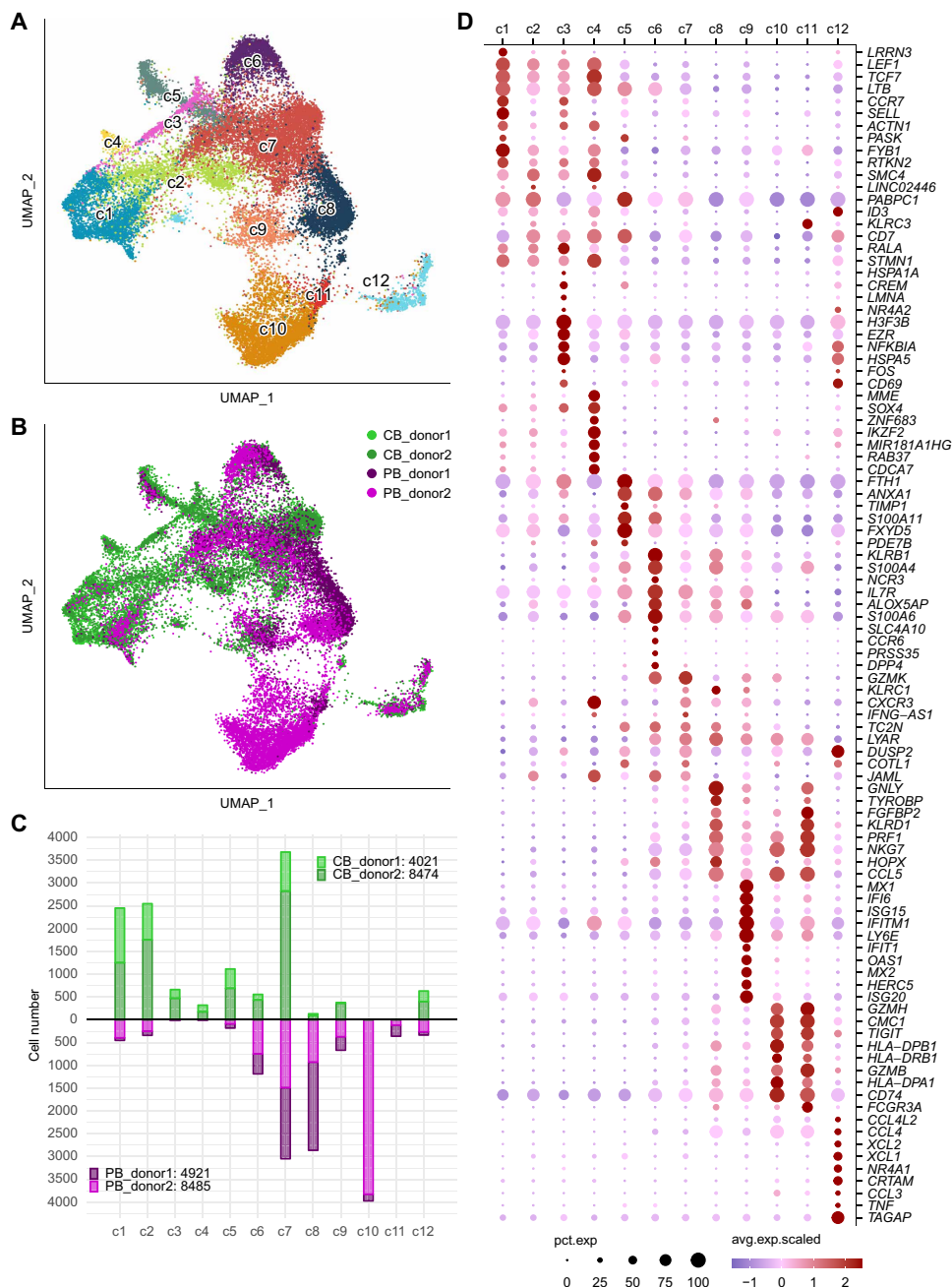
Fig. 1. scRNA-seq reveals high heterogeneity among human γδ T cells. Single-cell transcriptome libraries were generated from FACS-sorted γδ T cells of neonatal CB (CB_donor1 and CB_donor2; *n* = 2) or adult PB (PB_donor1 and PB_donor2; *n* = 2). (**A** and **B**) UMAP was adopted for visualization of cells. Each point represents a single cell. (A) Individual cells of all four donors are colored by clusters (c1 to c12) that were obtained from unsupervised clustering. (B) Individual cells are color-coded by donors. (**C**) The bar plot reveals fractions of absolute cell numbers from each donor that contributed to c1 to c12. Total cell numbers of donors that were considered for analysis are indicated in the figure legend. (**D**) The dot plot shows the top 10 up-regulated DEGs (rows) per cluster. Gene expression values were scaled to a log₂ fold change (logFC). Dots are colored by average logFC and sized by percentage of cells per cluster that expressed this gene (pct.exp). DEGs in this study are defined as follows: (i) absolute value of average logFC ≥ 0.25, (ii) adjusted *P* (adj.p) ≤ 0.01 (bimod test), and (iii) detected on at least 10% of cells from at least one cluster (min.pct ≥ 10%).

96.13% of the large cluster c10 originated from PB_donor2, indicating individual variances of phenotypes (Fig. 1C). However, all four donors contributed to all 12 clusters (fig. S2B). The dot plot of the top 10 differentially expressed genes (DEGs) in each cluster demonstrates the distinct gene expression profiles of each cluster (Fig. 1D). Among the 2308 DEGs, we found T cell–related regulatory transcription factors (TFs), cytokine receptors, cytotoxic genes, T cell activation genes, and NK cell receptors (fig. S2C).

Paired γδTCR analysis reveals mixed, Vγ9Vδ2⁺, and Vδ1⁺ T cell clusters

To add a further layer of information and link the scRNA-seq profiles of γδ T cells to individual γδTCR clones, a barcoded full-length complementary DNA (cDNA) library generated from single-cell RNA was split to generate additional libraries of scTCR-seq amplicons. To this end, we designed gene-specific primers within the 5′ region of the *TRGC* and *TRDC* segments, then amplified, and sequenced barcoded full-length V(D)J regions of the rearranged *TRG* and *TRD* genes. Shared cellular barcodes allowed us to assign individual *TRD* sequences to >80% of barcodes (single-cell transcriptomes) detected in the gene expression dataset, and clonal *TRG* and *TRD* pairs to about 45 to 70% of all single γδ T cell transcriptomes (fig. S3A). Mapping γδTCR clones to the clusters defined by UMAP in Fig. 1A highlighted a notable correlation of γδ T cell function to the rearranged V segments used to build γδTCRs (Fig. 2, A and B, and fig. S3B). The 12 clusters identified by scRNA-seq were largely grouped according to the distribution of individual TCR clones into three main sections. The neonatal γδ T cell–dominated clusters (c1 to c4) consisted of a heterogeneous mix of *TRG* and *TRD* combinations, including *TRGV9* paired with *TRDV2* (*GV9 DV2*), as well as clones using other segments such as *GV3 DV1*, *GV2 DV1*, and *GV3 DV3*. The second group, clusters c5 to c9, largely used pairs of *GV9* and *DV2* to build Vγ9Vδ2⁺ TCRs, whereas the adult γδ T cell clusters c10 and c11 as well as the mixed neonatal/adult cluster c12 were dominated by γδTCR using *DV1* (Fig. 2, A and B, and fig. S3B). Because activation, differentiation, and acquisition of effector function of γδ T cells are hypothesized to relate to cell proliferation, we examined clonal γδ T cell expansions based on the distribution of individual γδTCRs across the cell clusters

(Fig. 2C). The highest frequencies of individual γδTCR pairs with >100 cells per clone were found in adult PB *DV1*-dominated clusters c10 and c11, as well as among the Vγ9Vδ2⁺ TCR clones in *c7* to *c9* (fig. S3C). We calculated the repertoire diversity of each cluster in each donor based on paired γδTCR by Gini indices that ranged from 0 (completely polyclonal) to 1 (monoclonal) (Fig. 2D). In general, adult blood–derived γδ T cells showed a focused oligoclonal γδTCR repertoire (high Gini indices) in clusters constituted of both Vγ9Vδ2⁺ and non-Vγ9Vδ2⁺ TCR, whereas neonatal repertoires were polyclonal (lower Gini indices) (*11, 12, 24*). Specifically, immature γδ T cells of c1 to c4 from neonates and c1 from adults
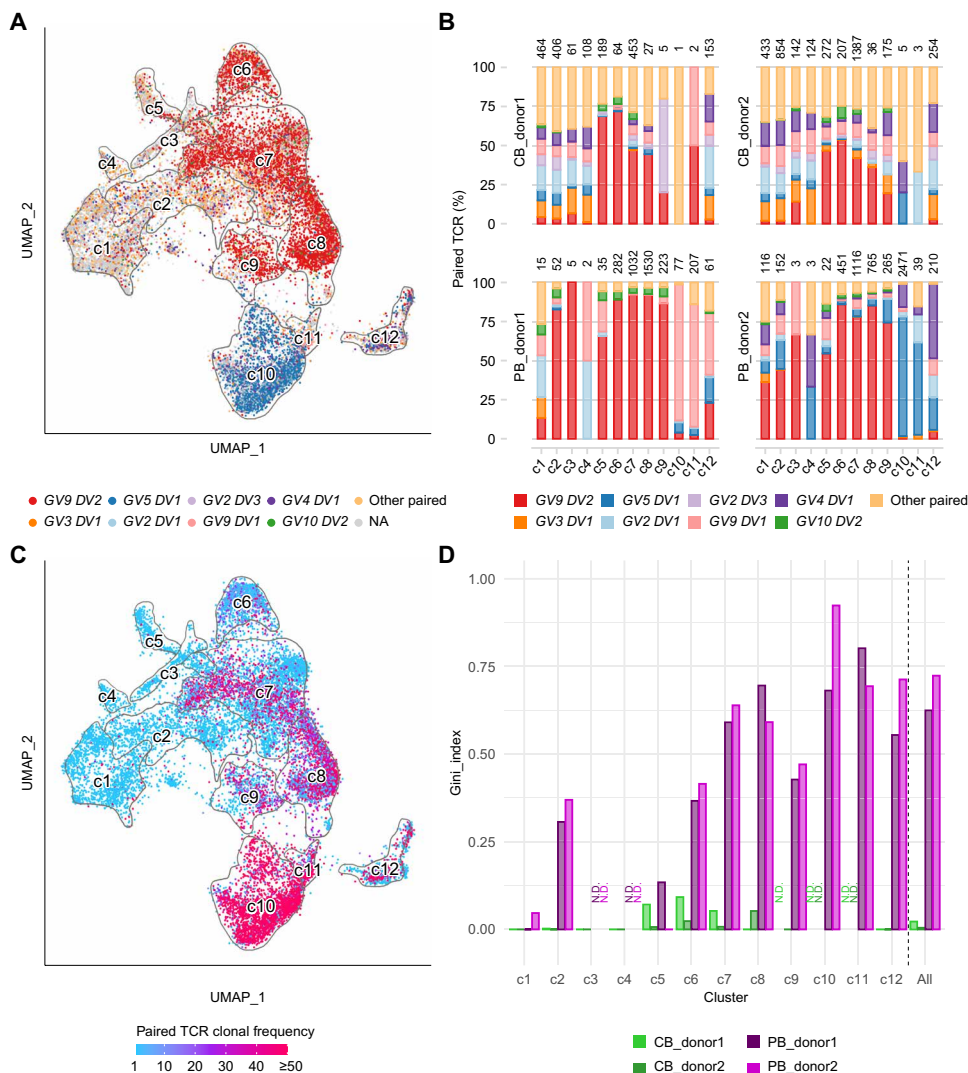
Fig. 2. scTCR repertoire analysis of clusters defined by scRNA-seq. Full-length γδTCR V(D)J segments were amplified from cDNA of scRNA-seq libraries (*n* = 4). Single-cell γδTCRs and single-cell transcriptomes were matched via cellular barcodes. (**A**) UMAP of γδ T cells shows paired γδTCR V gene usage (*TRGV* and *TRDV*). The most abundant pairs are color-coded (NA: paired TCR data are not available). Contours outline clusters c1 to c12 defined in Fig. 1A. (**B**) Bar plots depict paired γδTCR compositions in each cluster per donor. Cells without a productive paired γδTCR were excluded. The total numbers of paired γδTCR per cluster are indicated at the top of each bar. (**C**) The frequency of each identified paired γδTCR clone was calculated and visualized within the UMAP of γδ T cells. Cells without a paired γδTCR were excluded. (**D**) Single-cell paired TCR repertoire diversities were estimated by Gini indices that range from 0 (completely polyclonal) to 1 (completely monoclonal). Bar plot shows Gini indices of each donor within the respective cluster (c1 to c12) and total single-cell transcriptomes (all clusters per donor). Clusters containing less than 20 paired TCRs were excluded from Gini analysis and defined as N.D. (no data).

showed no clonal expansions with Gini indices close to zero (Fig. 2D). c10 cells of PB_donor2 (Fig. 1B) were largely constituted of a single *GV5 DV1* clone exclusively originating from the adult PB_donor2 (fig. S3C), indicating that these cells had likely undergone antigen-specific clonal expansion. In sum, we designed a paired *TRG/TRD* scTCR-seq approach to introduce a critical layer of information to our γδ T cell scRNA-seq data and segregated the 12 γδ T cell clusters into diverse immature and more differentiated Vγ9Vδ2⁺ clusters, as well as a non-Vγ9Vδ2⁺ TCR cluster that differed in their clonal compositions.

Gene coexpression modules delineate the functional diversity of γδ T cells

To further understand how heterogeneous gene expression patterns within the identified clusters reflected their potential functional commitment, we subjected the top 100 DEGs of each cluster (711 DEGs in total) to unsupervised clustering based on their average expression per cluster. This analysis identified eight gene coexpression modules (GMs) (Fig. 3, A and B, and table S1), which were annotated by selected key DEGs and Gene Ontology enrichment analysis (Fig. 3C). To understand how the 12 identified clusters were interwoven, vice versa modular scoring revealed the differential expression of these GMs among the 12 γδ T cell clusters defined above (Fig. 3B). Specifically, gene module A (GM_A) represented an immature naïve state of T cell differentiation and was enriched within most of the neonatal γδ T cells (c1, c2, and c4). GM_A included genes such as *LEF1* and *TCF7* that are key regulators of naïve T cells (*25, 26*) and known regulatory TFs of murine immature γδ T cells (e.g., *SOX4*) (*15, 27*). GM_B represented cell proliferation–associated genes with the highest score in c3. The innate T cell differentiation gene module GM_C was strongly present in c5, which contained mainly CB-derived Vγ9Vδ2⁺ cells. GM_C comprised the type 2 immunity–related genes *CD40LG* and *CCR4*, as well as the TF *ZBTB16* (PLZF), described to be critical for the development of invariant NKT cells and mucosal-associated T cells (*28, 29*). Of note, the type 3 immunity–related gene module GM_D, characterized by gene signatures connected to IL-17–producing T cells (*15, 29–31*), was exclusively enriched within c6, which contained neonatal and adult Vγ9Vδ2⁺ cells. Further modules enriched in Vγ9Vδ2⁺ cell clusters were GM_E with IFN type I signaling–related genes in c9 and GM_F with a set of NK cell–related (*KLRC1* and *KLRD1*) and

cytotoxicity (CTL)–related genes (*GNLY* and *GZMA*) in c8. Non-Vγ9Vδ2⁺ cell clusters c10 and c11 expressed GM_G characterized by a different set of cytotoxic T lymphocyte (CTL)–related genes (*TIGIT, BATF, EOMES, CD8A,* and *CD8B*). Last, GM_H indicated acute T cell activation in c12.

scRNA-seq of 25,904 human γδ T cells from CB and adult PB revealed a high functional heterogeneity with common and distinct cell transcriptional patterns among neonatal and adult γδ T cells. Detailed analysis of DEGs identified key core GMs that defined γδ T cell differentiation to functional subsets including CTL activity and type 3 immunity, which largely correlated with clonal expansion of either Vγ9Vδ2⁺ or non-Vγ9Vδ2⁺ T cells.

Fig. 3. Identification of GMs from single-cell transcriptomes. Top 100 DEGs in all clusters (TCR, ribosomal, and mitochondrial genes excluded, 711 DEGs in total) were subjected to unsupervised clustering based on the average DEG expression per cluster (c1 to c12), and eight GMs were identified. Annotation of the eight GMs was supported by Gene Ontology enrichment analysis. (**A**) The DEGs were enwrapped by UMAP and colored by modules. Each dot represents a DEG. Selected key DEGs are labeled. (**B**) The heatmap depicts the modular scores of each cell. Cell numbers were downsampled to a maximum of 600 cells per cluster. (**C**) Gene Ontology enrichment analysis on GMs. Each dot represents an enriched Gene Ontology term, which is colored by adjusted *P* value and sized by enrich-fold, respectively. MHC, major histocompatibility complex; NF-κB, nuclear factor κB.

Vγ9Vδ2⁺ T cells are innate-like T cells with TCRs enriched in public sequences

We investigated the link between Vγ9Vδ2⁺ TCR clonotypes and functional differentiation of Vγ9Vδ2⁺ T cells. Nearly all Vγ9Vδ2⁺ T cells expressed genes that guide lineage commitment of innate-like T cells, including canonical Vγ9Vδ2⁺ T cells (*17, 32*), namely *ZBTB16* (encoding PLZF), *KLRB1* (encoding CD161), and *KLRC1* (encoding NKG2A), albeit at different levels (Fig. 4A). However, it is still unclear how far postnatal selection shapes the repertoire of adult Vγ9Vδ2⁺ T cells (*33, 34*). Deep sequencing analyses of bulk *TRG* repertoires established a high frequency of shared and thus "public" *TRGV9* sequences in neonatal and adult blood samples (*11, 12, 35*), but it is thought that the corresponding *TRDV2* sequences are rather diverse and lead to individual and thus "private" repertoires of semi-invariant Vγ9Vδ2⁺ T cells.

We compared the 4052 individual *TRDV2* gene clones from this scTCR-seq analysis to *TRD* repertoires obtained by previous bulk TCR sequencing of γδ T cells from 80 independent donors (*11, 18, 36*) to determine the frequency of Vγ9Vδ2⁺ T cells using shared public *TRDV2* sequences. We noticed that most of all Vγ9Vδ2⁺ T cells in clusters c5 to c9 displayed public *TRDV2* gene rearrangements, such that exactly the same *TRDV2-CDR3* sequences were shared between individual donors (Fig. 4B and fig. S4, A and B). In contrast, almost all other *TRD* clones were private and did not share their unique *TRDV-CDR3* between individuals (fig. S4A). Furthermore, Vγ9⁺ T cells of clusters c5 to c9 showed *TRGV9/TRGJP* rearrangements with little clonal diversity (fig. S4C). Together with previous studies investigating the TCR repertoire and phenotype of Vγ9Vδ2⁺ T cells (*9, 11, 17, 22, 24, 33–37*), the innate-like transcriptional program and usage of largely public clonotypes characterize Vγ9Vδ2⁺ T cells as genuine innate-like T cells.

Identification of a distinct type 3 immunity–committed Vγ9Vδ2⁺ γδ T cell subset

A number of genes were differentially expressed among the Vγ9Vδ2⁺ T cell clusters (Fig. 4C and fig. S4D) despite apparent similarities. The mostly CB-derived Vδ2⁺ T cells of c5 expressed *CCR4* and *CD40LG*, which are relate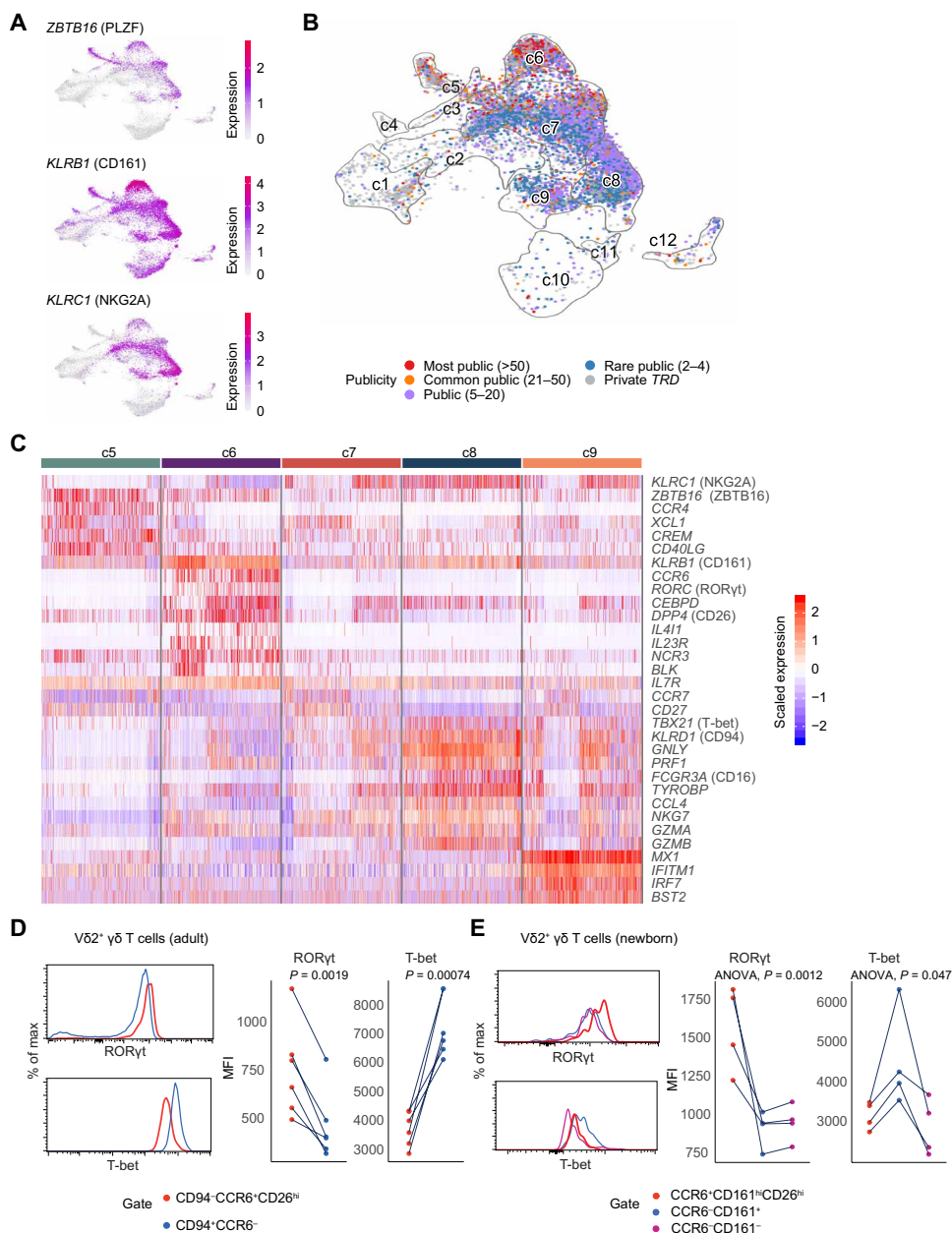d to type 2 immunity (*38*). In contrast, the mostly adult-derived Vγ9Vδ2⁺ T cells in c8 expressed *KLRD1* (encoding CD94), type 1 immunity signature genes such as *TBX21*, and genes related to cytotoxicity—including *FCGR3A* (encoding CD16), *PRF1*, and *GZMA*—suggesting differential roles of innate-like

Fig. 4. Vγ9Vδ2⁺ T cells are innate γδ T cells with TCRs enriched in public *TRD* sequences. In-depth analysis focusing on neonatal and adult Vγ9Vδ2⁺ T cell clusters defined in Fig. 2. (**A**) Visualization of *ZBTB16* (PLZF), *KLRB1* (CD161), and *KLRC1* (NKG2A) expression on γδ T cells (adopted from fig. S2C). (**B**) UMAP of Vδ2⁺ γδ T cells with delineation of respective clusters (from Fig. 1A) projects the publicity of Vδ2 *TRD* repertoires per cluster. Bulk *TRD* repertoires (ranging from infants to adults, *n* = 80) were compared with the four scTCR-seq libraries of this study. Publicity was defined by being present in the respective number of donors, indicated in parentheses of the legend. (**C**) Expression levels of selected DEGs are visualized by heatmap on c5 to c9. (**D** and **E**) FACS of RORγt and T-bet expression on Vδ2⁺ γδ T cells from adult PB (D) or CB (E). Vδ2⁺ γδ T cells were gated by CD94, CCR6, CD26, and CD161 as presented in fig. S5. Median fluorescent intensity (MFI) was used for statistics; paired Student's *t* test or one-way analysis of variance (ANOVA) test was performed, and exact *P* values are stated for (D) and (E), respectively. Data are representative of two independent experiments, and each dot represents one donor.

Vγ9Vδ2$^+$ T cells in the neonatal and adult immune system. Clusters c6, c7, and c9 were composed of Vγ9Vδ2$^+$ T cells derived from both cord and adult blood donors. Of those, c7 cells displayed gene expression profiles of naïve T cells (CCR7 and CD27), and c9 cells were enriched in IFN-induced genes (MX1, IFITM1, and IRF7). c6 cells expressed a type 3 immunity/T helper 17 (T$_H$17)–related gene signature including CCR6, RORC, IL23R, and DPP4 (encoding CD26) (Figs. 2B and 4C and fig. S4, D and E). Because the translation of RORC to RORγt protein and the functional potential to produce IL-17 cytokines are an area of debate for human γδ T cells (10, 30), we picked several key signature genes to delineate and sort Vδ2$^+$ T cells by flow cytometry for functional analysis. Figure S5 (A and B) displays our gating strategy of Vδ2$^+$ T cells into CCR6$^+$CD161^{hi}CD26^{hi} (representing neonatal and adult c6 cells), CCR6$^-$CD161$^+$CD26$^-$ (representing neonatal c7 cells), and CCR6$^-$CD161$^-$CD26$^-$ subsets (representing neonatal c5/c1 cells), as well as CD94$^+$CCR6$^-$ cells that are exclusively found in adults (representing c7 and c8 cells). RORγt expression was evident in adult CD94$^-$CCR6$^+$CD26^{hi} Vδ2$^+$ cells, whereas CD94$^+$CCR6$^-$ Vδ2$^+$ T cells were T-bet positive (Fig. 4D). In CB, we found RORγt expression in CCR6$^+$CD161^{hi}CD26^{hi} Vδ2$^+$ T cells, and only neonatal CCR6$^-$CD161$^+$ Vδ2$^+$ T cells showed moderate levels of T-bet expression (Fig. 4E).

To directly test whether human type 3 γδ T cells were biased toward an IL-17 cytokine profile, we adopted a protocol to culture and stimulate CB mononuclear cells (CBMCs) under T$_H$17-polarizing conditions (39–41). Efficiency of induction of IL-17 production varied between individual donors, and IL-17 production could be induced in some γδ T cells of the type 3 CD94$^-$CCR6$^+$CD26$^+$ Vδ2$^+$ T cell subset (fig. S5C), but IFN-γ expression was mostly limited to CCR6$^-$ Vδ2 T cells. To verify that the ex vivo culture would stimulate human type 3 γδ T cells to produce IL-17 rather than just inducing "naïve" undifferentiated γδ T cells to adopt a type 3 γδ T cell phenotype, we sorted CBMC-derived γδ T cells into CD94$^-$CCR6$^+$CD26$^+$ and CCR6$^-$ Vδ2 T cells before culture with irradiated autologous CBMCs (fig. S5, D and E). We observed very few IL-17–producing γδ T cells specifically within the CCR6$^+$-sorted cultures. Most of the IFN-γ–producing cells were CCR6$^-$, and CCR6$^+$ expression could not be induced in CCR6$^-$-sorted cells. In sum, these data support the hypothesis that CD94$^-$CCR6$^+$CD26$^+$ Vδ2$^+$ cells comprised in c6 represent precommitted innate type 3 γδ T cells that are conserved among neonates and adults.

To investigate the clonal relationship of all clusters containing adult Vγ9Vδ2$^+$ T cells, we calculated the overlap of identical GV9/DV2 sequence pairs in clusters c2 and c6 to c9. The phenotypically naïve/resting clusters (c7 and c2) shared 44 to 100% of their clones in both adult samples with the effector clusters (c8 and c9), whereas their overlap with type 3 immunity–related c6 cells was much less detectable (Fig. 5A), suggesting the use of distinct TCR clonotypes/sequences in cluster c6. The 10 most expanded (top 10) Vγ9Vδ2$^+$ TRD clones from cluster c6 of both adult samples were much less connected with the top 10 clones in c2 and c7 to c9, but those four clusters shared at least 3 of their top 10 clones within both donors (Fig. 5B). To further substantiate these clonal relationships between functional subsets of Vγ9Vδ2$^+$ T cells, we sorted Vγ9Vδ2$^+$ T cells from PB of additional four unrelated adult donors according to the expression of their cluster-defining DEGs CD94, CCR6, CD16, and CD26 (fig. S6A). In this scheme, c6 cells corresponding to CD94$^-$CCR6$^+$CD26$^+$ (type 3 γδ T cells) showed very little overlap to CD94$^+$CCR6$^-$ populations of Vγ9Vδ2$^+$ T cells (corresponding to c7 and c8) as defined

by bulk TRD repertoire sequencing (fig. S6B). Our analyses support the view that type 3 immunity–related γδ T cells of cluster c6 cells have a distinct TCR repertoire with high levels of public TRDV2 sequences, express key signature genes of innate-like T cells and type 3 immunity, and may have a distinct early ontogenetic origin reminiscent of γδT17 cells in mice that emerge during a defined window of fetal development and are prewired to produce IL-17 (14, 31, 42).

Human type 3 γδ T cells originate from the earliest embryonic thymocytes

We tested whether human γδ T cells with a type 3 immune phenotype similar to cluster c6 and defined by gene module GM_D (Fig. 3A) arise during early human ontogeny by using a recent scRNA-seq study that resolved human thymus organogenesis in the embryonic weeks 8 to 10 (Ewk8 to Ewk10) (43). Reanalysis of this dataset [Gene Expression Omnibus (GEO): GSE133341] identified four thymic γδ T cell clusters (here labeled as gdT_1 to gdT_4) according to CD3D and TCR gene expression (Fig. 6A and fig. S7, A and B). Two smaller γδ T cell clusters (gdT_3 and gdT_4) originated exclusively from Ewk8 and Ewk9 thymi, but the two larger γδ T cell clusters (gdT_1 and gdT_2) mainly arose from Ewk9 and Ewk10 thymocytes (Fig. 6B). Comparison of the expression of five relevant gene modules identified above (Fig. 3 and table. S1) to this dataset of embryonic thymocytes indicated that most of the Ewk10 γδ T cells (gdT_1 and gdT_2) and the αβ T cell clusters could be distinguished by gene modules of naïve and immature T cells (GM_A) (Fig. 6C). In contrast, gdT_3 and gdT_4 γδ T cells, which were enriched in Ewk8 and Ewk9, showed strong expression of the innate T cell differentiation gene module (GM_B). Moreover, the gdT_3 and gdT_4 clusters were separated by CTL response (γδT_4) and type 3 immunity (gdT_3) gene modules (Fig. 6C). The heatmap in Fig. 6D highlights the differential expression of cytotoxicity-related genes (e.g., KLRD1, PLAC8, NKG7, TYROBP, and GZMA) on cluster gdT_4 and of type 3 immunity signature genes (e.g., RORC, CCR6, and IL23R) on cluster gdT_3. We speculate that those cells mainly consist of Vγ9Vδ2$^+$ T cells because TRGV9 is enriched in clusters gdT_3 and gdT_4, and a previous study indicated that fetal T cells between 7 and 11 weeks of development are primarily Vγ9Vδ2$^+$ T cells (16). Both subsets expressed ZBTB16 (encoding PLZF) and KLRB1 (encoding CD161), two genes previously described on fetal blood Vγ9Vδ2$^+$ T cells (17). Expression of CD44 and CD69 and the absence of immaturity genes, including SOX4, LEF1, TCF7, and PTCRA (coding for pre-TCRα in immature T cell precursors), further suggested that these two γδ T cell clusters gd_3 and gd_4 were not composed of developing early thymocytes but rather of mature postselection T cells (Fig. 6D).

Human cluster gdT_3 cells were exclusively present in the human thymus at Ewk8 and Ewk9 but not at Ewk10. Their transcriptional patterns point toward an early thymic functional precommitment of type 3 γδ T cells that may persist into adulthood as cluster c6 cells, which resembles the ontogeny of γδT17 cells in mice.

Vδ1$^+$ γδ T cells mature into PD1^{hi} and PD1^{low} cells

Next, to understand the effector differentiation associated with clonal expansion of adult Vδ1$^+$ T cells, we analyzed their transition from immature to effector Vδ1$^+$ T cells at the transcriptional level. Neonatal and adult Vδ1$^+$ T cells of c1 were dominated by the gene module of naïve and immature T cells (GM_A) and expressed
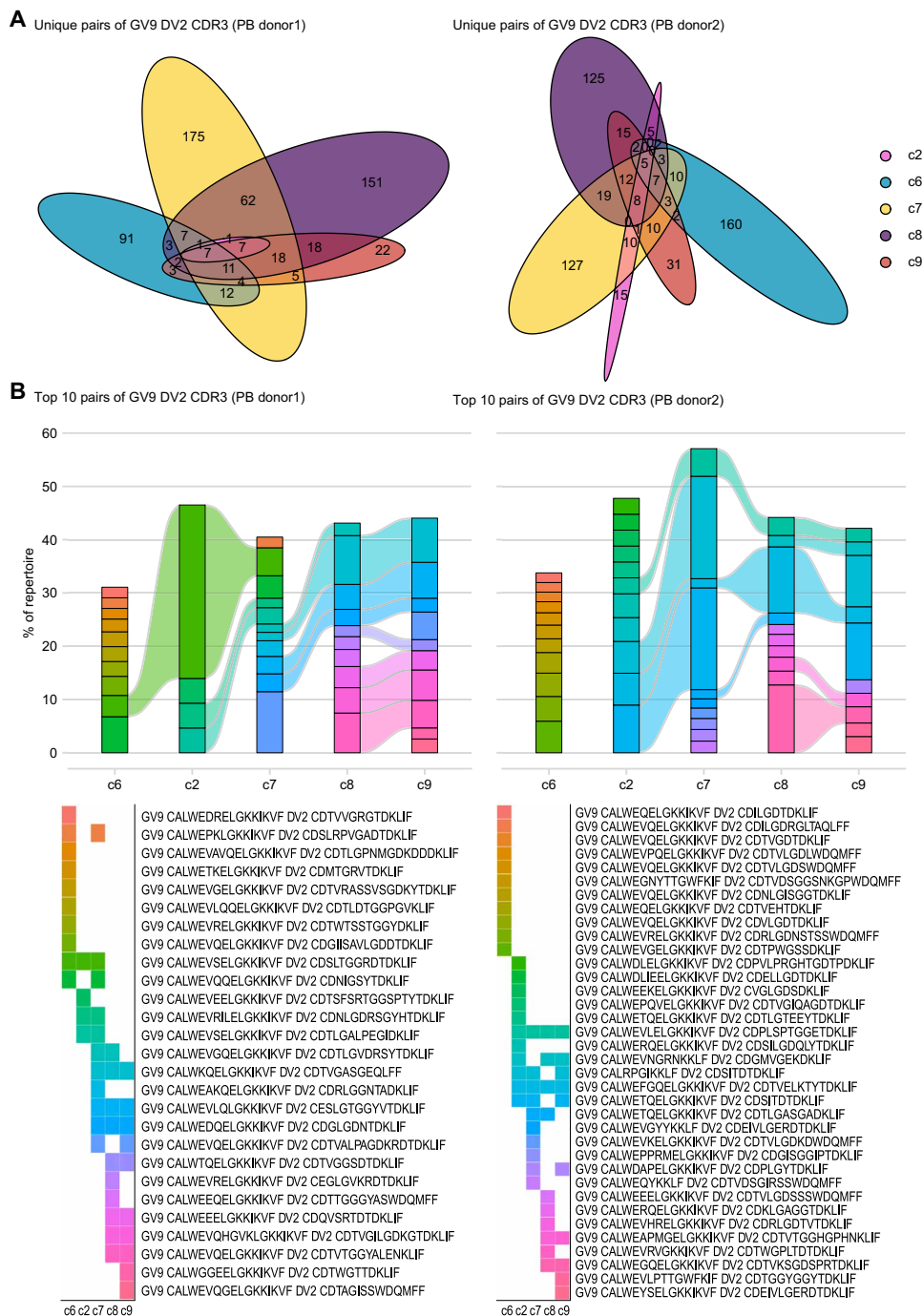
Fig. 5. Innate type 3 γδ T cells show distinct Vγ9Vδ2+ TCR repertoire profiles. Vγ9Vδ2+ TCR repertoires of innate type 3 γδ (c6), innate type 1 (c7 to c9), and naïve T cell (c2) phenotypes were investigated in adult PB_donor1 and PB_donor2. (**A**) Overlap analysis of paired TCR clones was performed for PB_donor1 and PB_donor2. The amount of overlapping clones among clusters is visualized and described in Venn diagrams, and the size of the ellipse reflects the number of unique TCR clones in each cluster. (**B**) The 10 most expanded Vγ9Vδ2+ TCR clones (top 10) from clusters c2 and c6 to c9 were selected for overlap analysis. The colored bands between columns represent shared clones among clusters. The order of clusters was adjusted for visualization. Results for PB_donor1 are on the left side and for PB_donor2 on the right side. (A and B) Cluster c5 was excluded from the analysis because too few cells originated from adult donors.

$CCR7$, $CD27$, and $IL7R$ (Figs. 3, A and B, and 7, A and B), but Vδ1+ T cells in c12 showed gene expression profiles of acute activation (GM_H) (Figs. 3, A and B, and 7A). $CCR9$ expression was constrained to a fraction of these neonatal γδ T cells, suggesting that they might have recently emigrated from the thymus (Fig. 7A) (44–46). Adult effector Vδ1+ T cells (c10 and c11) were controlled by a Vδ1+ T cell–specific gene core module of CTL responses (GM_F) including $TBX21$, $EOMES$, $CD8A$, $CD8B$, and granzyme genes (Figs. 3, A and C, and 7A). Cells within c10 expressed signature genes such as $PDCD1$ (encoding PD1), $IKZF2$, $HLA-DRA$, and moderate levels of $CD27$ and $IL7R$, whereas c11 was more enriched for NK receptors such as $KLRD1$ (CD94) and $KLRF1$ (NKp80) and cytotoxic genes such as $TYROBP$ and $FCGR3A$ (CD16) (Fig. 7, A and B). Gene set enrichment analysis (GSEA) further suggested that c10 and c11 matured into PD1^low and PD1^hi effector cells similar to terminally differentiated and effector memory CD8+ T cells from healthy donors (47), respectively (Fig. 7C). Mapping of unique paired CDR3γ/CDR3δ sequences from the two adult donors to the Vδ1+ clusters revealed that the terminally differentiated effector clones of c10 to c12 were highly overlapping within each donor but distinct from immature cells in c1 (fig. S8A).

To further characterize the differentiation of c10 and c11 Vδ1+ T cells, we introduced a flow cytometric surface marker staining strategy based on CCR7 and CD27 to delineate between clusters c1 (CCR7+CD27^hi), c10 (CCR7−CD27^int), and c11 (CCR7−CD27−) cells (Fig. 7D and fig. S8B). Combined analysis of Vδ1+ T cells from 10 adult healthy donors largely matched the scRNA-seq gene expression profiles of CCR7−CD27^int c10 cells as being PD1^hi with low CD94 and CD16 protein expression, whereas CCR7−CD27− c11 cells displayed intermediate PD1 levels and high expression of CD94 and CD16 (Fig. 7E). CCR7− CD27^int c10 and CCR7−CD27− c11 Vδ1+ T cells produced IFN-γ and tumor necrosis factor–α (TNFα) after short-term ex vivo stimulation (Fig. 7F), supporting the notion that both subpopulations are functional effector cells. Together, these data support a trajectory of Vδ1+ T cells from an immature/naïve state in

Delineating Vδ1[+] and Vδ2[+] effector subsets via flow cytometry

The combination of scRNA-seq and scTCR-seq identified distinct phenotypes of human γδ T cells, including type 3 immunity–related Vγ9Vδ2^{+} T cells, in CB and adult PB. To validate and to apply these results to a larger number of samples than it is feasible by scRNA-seq, we selected nine differentially expressed indicator surface markers that represented the phenotypes and gene modules of γδ T cells for validation by flow cytometry (fig. S9). In addition to antibodies specific for Vδ1[+], Vδ2[+], and pan-γδTCR, the panel included nine antibodies directed against CCR7 and CD127 (*IL7R*) for central memory and naïve phenotypes; CCR4 to identify type 2 immunity–related Vγ9Vδ2^{+} T cells; CD161 (*KLRB1*), CCR6, and CD26 (*DPP4*) as markers for type 3 immunity–related Vγ9Vδ2^{+} T cells (*41, 48*); CD94 (*KLRD1*) and CD16 (*FCGR3A*) representing CTL activity; and PD1 (*PDCD1*) to delineate different effector Vδ1[+] γδ T cell subsets. With this simplified approach, we could successfully validate and reproduce the presence of similar γδ T cell subsets in independent cord and adult blood donors. On the basis of the combined flow cytometric analysis of five CB and six adult blood samples by UMAP and unsupervised clustering, we identified 10 distinct clusters (named FACS1 to FACS10) that largely corresponded with the 12 clusters identified by scRNA-seq (Fig. 8, A and B, and fig. S10, A to C). Dimensional reduction was performed on the basis of only nine selected surface markers, but the "FACS clusters" obtained from this analysis comprised either (immature) mixed Vδ1[+,] and Vδ2^{+} T cells or only Vδ1[+] or Vδ2^{+} T cells (Fig. 8C), similarly to total scTCR-seq analyses (Fig. 2A). γδ T cells allocated to distinct clusters according to their origin from neonatal or adult donors (Fig. 8D and fig. S8A) in the same way as observed by scTCR-seq analyses (Fig. 1B). A notable example of a γδ T cell subset that was present in both neonate and adult samples was cluster FACS6, representing CCR6^{+}CD26^{+}CD161^{+}Vδ2^{+} γδ T cells (type 3 γδ T cells). The phenotype, composition, key markers, and interrelatedness of γδ T cell clusters defined by flow cytometry versus scRNA-seq are summarized in Fig. 8E. Briefly, the flow cytometry panel comprising three γδTCR and nine surface molecule markers not only

Fig. 6. γδ T cells acquire effector phenotypes during early fetal thymic development. Single-cell transcriptome dataset of thymi from Ewk8 to Ewk10 was acquired from GEO (*43*), GEO: GSE133341. T cells (defined by *CD3D* expression in fig. S7A) were subjected to this reanalysis. (**A**) UMAP illustrates unsupervised clustering results of embryonic thymocytes. Names of clusters were determined by the expression of TCR genes (fig. S7B). (**B**) UMAP describes the origin (embryonic week) of thymocytes via respective color codes. (**C**) GM (defined in Fig. 3) modular scores of embryonic thymocytes are shown by violin and box plots. The three horizontal lines of the box-whisker plot represent the higher quartile, median, and lower quartile, respectively. (**D**) Representative key DEGs among fetal thymus T cells are presented in the heatmap. Cells were downsampled to a maximum of 200 cells per cluster.

c1 over acute activation in c12 to differentiate into several flavors of differentiated effector cells, i.e., PD1^{low} Vδ1[+] γδ CTLs (c11) or PD1^{hi} Vδ1[+] γδ T cells (c10).

We addressed whether these type 3 γδ T cells comprised in cluster c6/FACS6 could be generated de novo from hematopoietic stem cells in the human postnatal thymus by applying our FACS (fluorescence-activated cell sorting) panel to analyze the PB γδ T cells of three adult individuals with inborn *IL2RG*-deficient severe combined immunodeficiency (SCID), who were transplanted with *IL2RG*-sufficient T cell–depleted bone marrow at the age of 1 year (fig. S10D). In line with previous reports (*49*), Vγ9⁺CCR6⁺ T cell frequencies were highly heterogeneous in healthy control donors but were very low or even undetectable in the reconstituted adult SCID patients at >20 years after bone marrow transplantation.

DISCUSSION

In this work, the combination of scRNA-seq and scTCR-seq of sorted adult and neonatal γδ T cells allowed us to establish a comprehensive map of γδ T cell phenotypes and to associate them to paired γδTCR sequences. Functional diversity of human γδ T cells, as monitored by DEGs, largely correlated with the type of γδTCRs expressed in each cell. Polyclonal neonatal cells dominated the more naïve clusters (c1 to c4), characterized by expression of genes involved in innate T cell differentiation, and the other clusters (c5 to c12) showed distinct patterns of T cell activation, proliferation, and lineage-specific differentiation. Furthermore, we extracted eight GMs (*26*, *27*) that characterized the naïve, proliferating, acutely differentiating, type 3 immunity, IFN-induced, cytotoxic, and acute activation phenotypes in human γδ T cells. Compositions of naïve, IFN-induced, and cytotoxic GMs mostly resembled those identified from human αβ T cells (*26*), but γδ T cells have their own biology. Several reports have used αβ T cell–associated terms to describe human γδ T cells as central memory, effector memory, and TEMRA (*50*, *51*), but it should not be assumed that they follow the same trajectories during their maturation to effector T cells. Differences between αβ and γδ T cell differentiation and homeostasis are apparent when it comes to

Fig. 7. Vδ1⁺ γδ CTLs mature into PD1ʰⁱ and PD1ˡᵒʷ cells. Cell clusters with high *TRDV1* gene expression (from Fig. 2; c1 and c10 to c12) were further analyzed. (**A**) The heatmap describes selected DEGs among clusters c1 and c10 to c12. (**B**) Expression levels of DEGs plotted by violin and scatterplots. (**C**) GSEA was performed between c10 and c11 referring to the immunological gene sets of the Molecular Signatures Database (www.gsea-msigdb.org). The enriched terms were from GEO (GSE26495). (**D** and **E**) FACS analysis of Vδ1⁺ γδ T cells by CCR7, CD27, IL7R, PD1, CD94, and CD16 (bulk data combined from *n* = 10 donors and individual analyses). (D) Vδ1⁺ γδ T cells are positioned and gated by CCR7 and CD27 expression. (E) Cells positioned by CCR7 and CD27 are colored by scaled fluorescent intensities of IL7R, PD1, CD94, and CD16, respectively (E) (top). Biexponential median fluorescent intensity values were used for statistics; each dot in the dot plot represents one donor (E) (bottom). (**F**) TNFα and IFN-γ production after PMA/ionomycin stimulation was measured on Vδ1⁺ γδ T subpopulations defined in (D). Vδ1⁺ γδ T are further gated by TNFα and IFN-γ cytokine production. The numbers in the four corners indicate the mean percentage and SD (*n* = 10). (D to F) Fluorescent intensities used in FACS analysis by R were biexponentially transformed.

validates our scRNA-seq data but also provides a strategy to monitor the diverse γδ T cell subsets identified in neonatal and adult blood.

adaptive immunity and T cell memory. There is good evidence that Vδ1⁺ undergo clonal expansion in response to viral infection (*11*, *12*), but the involved antigens are largely unknown. Those expanded γδ
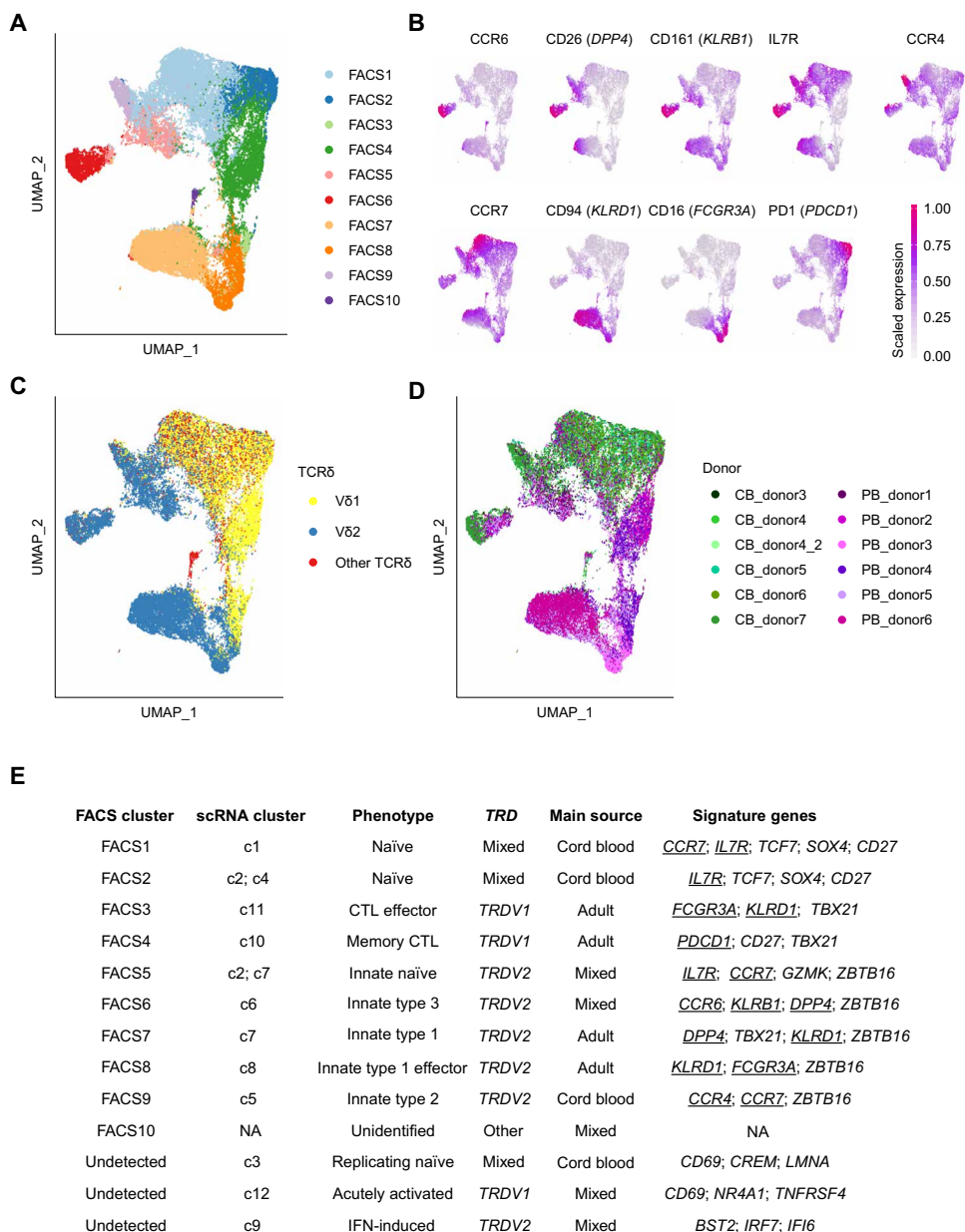
Fig. 8. Flow cytometry analysis delineates Vδ1+ and Vδ2+ naïve and effector γδ T cell subsets. γδ T cells from five CB and six adult PB donors were subjected to FACS analysis. CB_donor4_2 was an independent replicate of CB_donor4 to control the batch effects. PB_donor1 and PB_donor2 were identical to adult donors of scRNA-seq data. γδ T cells were stained by pan-γδTCR, Vδ1, and Vδ2 antibodies, and nine lineage markers were included. Fluorescence intensities used in FACS analysis by R were biexponentially transformed. (**A**) FACS data of γδ T cells were subjected to unsupervised clustering and enwrapped by UMAP. Each point represents a single cell and is color-coded by FACS cluster. (**B**) Expression values of the nine lineage markers were scaled to a range between 0 and 1 and projected on UMAP. (**C** and **D**) Individual cells are color-coded by (C) corresponding TCRδ chains or (D) donor ID. Gating of Vδ1+ and Vδ2+ T cells is shown in fig. S10B. (**E**) Overview of the corresponding clusters from multicolor FACS analysis and scRNA-seq. Phenotypes sources, TCRδ usage, and corresponding signature genes are summarized in the table. The nine lineage markers selected for FACS validation are underscored.

T cell clones do not contract after an immune response and thus form distinct memory T cell populations such as CD8+ T cells. Comparison of cord and adult blood samples was consistent with findings that neonatal γδ T cells are more immature, less differentiated, and polyclonal (18, 34, 52), whereas adult γδ T cells are more activated

and show restricted clonality (11, 12, 53). At the same time, CB and early fetal thymus contained innate type 3 and type 1 immunity–related effector populations that could presumably persist into adulthood, sharing some, but not all, features with Lin28b-dependent effector γδ T cells, recently found in weeks 17 to 19 of fetal thymus (22).

The semi-invariant Vγ9Vδ2+ T cells clustered with each other by scRNA-seq, but they could be separated into immature and mature types with strong parallels to lineage-specific differentiation and acquisition of effector functions of other PLZF+ innate lymphocytes such as NKT-1, NKT-2, and NKT-17 cells (9, 10, 28, 54–57). Paired *TRG* and *TRD* scTCR-seq analysis was important to validate the segregation of these clusters, because certainly not all Vδ2 chains must pair with Vγ9 chains and vice versa (3, 11, 22, 24). In addition to the expression of the innate-like T cell marker PLZF, we found an unexpectedly high abundance of shared or public Vγ9Vδ2+ TCR clones among adult Vγ9Vδ2+ T cells, which firmly establishes their germline-encoded and evolutionarily conserved innate phenotype (18). We also observed committed type 1 and type 3 immunity–related Vγ9Vδ2+ cells in the earliest wave of thymus organogenesis, as well as in CB and adult blood samples. This is consistent with the hypothesis that human innate Vγ9Vδ2+ effector γδ T cells develop in early fetal waves and persist into adulthood, as it has been described for mouse γδT17 and γδT1 cells (14, 58). One outstanding question is why this subset has not been observed before. Timing might be critical for their detection, because effector Vγ9Vδ2+ cells are present very early in T cell ontogeny (16, 17) but hard to find in the later fetal thymus (weeks 17 to 19) (22) and absent in the postnatal thymus (21). The earliest innate PLZF+ type 3 γδ T cells and γδ type 1 cells probably leave the human fetal thymus and home to distant tissues after gestational week 9, in line with our detection of these cells in thymi of weeks 8 and 9 but not week 10. Such a strict fetal origin of effector cells is a defining feature of innateness and parallels the ontogeny of IL-17–producing lymphoid tissue–inducer cells that seed and persist in secondary lymphoid tissues (59). Likewise, PLZF expression maps the early stages of ILC1 lineage development (56).

Because the negligible production of IL-17 of human PLZF+ CCR6+CD26+CD161+ γδ T cells remains a major caveat, we propose

that it is appropriate to label them type 3 γδ T cells, but not γδT17, analogous to related populations in mice (*42*). Several reports identified that specific subsets of Vδ2[+], but not Vδ1[+], cells expressing IL-23R (*39*), CD161 (*41, 60*), or CCR6 (*41, 49, 61, 62*) are likely to produce IL-17 in humans. However, the protocols used to activate Vδ2^{+} cells in these reports relied on long weeks rather than days of in vitro culture in the presence of T$_H$17-polarizing stimuli, raising concerns whether this was differentiation rather than activation. It was noted that IL-17–expressing type 3 γδ T cells from CB were much more efficiently expanding than those from adult PB mononuclear cells (PBMCs) (*39, 63*). Reports of adult human γδ T cells from synovial fluid biopsies (*64*) or liver perfusions (*57*) that spontaneously secreted IL-17 cytokines after a brief (hours) ex vivo stimulation remain rare exceptions. Perhaps type 3 γδ T cells require a very specific set of environmental queues before eliciting a better response. Here, we define human type 3 immunity–related γδ T cells by expression of canonical Vγ9Vδ2[+] TCR and the gene expression module GM_D comprising *IL23R*, *RORC*, and *BLK*. CCR6 remains the most stringent single surface marker for human type 3 γδ T cells as also observed in mice (*65*). CCR6 expression could not be induced in sorted CCR6[−] cells in vitro under T$_H$17-polarizing conditions, and CCR6^{+} type 3 γδ T cells were inefficient IFN-γ producers as compared with CCR6^{−} γδ T cells. We propose that human CCR6^{+} γδ T cells, similar to mouse CCR6^{+} γδT17 cells (*14*), are preferentially or even exclusively generated early before birth and prone to type 3 immune responses. This hypothesis is supported by (i) our finding that adult *IL2RG*-deficient patients with SCID who were transplanted with *IL2RG*-sufficient T cell–depleted bone marrow postnatally lacked CCR6^{+} Vγ9^{+} T cells, (ii) the direct identification of these cells in published datasets of fetal thymus Ewk8 to Ewk9 but not Ewk10 (*43*), (iii) the presence of the type 3 immunity–biased cluster c6 cells in samples from the cord and adult blood, and (iv) paired TCR analyses revealing that c6 cluster γδ T cells showed unique TCR profiles different from the other Vγ9Vδ2[+] cell–dominated clusters and have an even more public TCR repertoire.

We present a multidisciplinary approach to comprehensively map functional human γδ T cell subsets and provide a FACS panel that can be easily implemented to reproduce this classification. This may help to decipher the factors that drive the composition of γδTCR clonotypes and functional γδ T cell subsets in humans and to understand whether these individual "γδ T cell-omes" can influence or predict how individuals will cope with neoplastic and infectious challenges.

MATERIALS AND METHODS
Study design
To investigate how distinct transcriptional programs of human γδ T cells are guided by their individual γδTCRs, we combined scRNA-seq of sorted γδ T cells from two unrelated CB and two unrelated adult PB samples with scTCR-seq using custom *TRGC* and *TRDC* gene-specific primers. We performed additional bulk TCR-seq of adult PB γδ T cells and validated our findings via multicolor flow cytometric analysis. In total, this study included 40 adult healthy PB donors, 18 CB donors, and PB from 3 adult individuals with inborn *IL2RG*-deficient SCID that received bone marrow transplantation during early childhood. The data were supported by reanalysis of public domain data, i.e., 80 additional *TRD* repertoires from bulk TCR-seq (*11, 12, 35*) and scRNA-seq data from human fetal thymus (*43*).

Human samples and isolation of mononuclear blood cells
Inclusion of healthy donors, patients, and CB donors in this study was performed in accordance with the Declaration of Helsinki and approved by the institutional ethics review board at Hannover Medical School (Hannover, Germany) under study numbers 1303-2012 (CB donors), 7600-2017 (patients), and 7901-2018 (adult healthy donors). All donors (parents in the case of CB donors) gave written informed consent before sample collection. PBMCs and CBMCs were isolated from fresh EDTA blood samples using density gradient media. After isolation, mononuclear cells were washed twice in phosphate-buffered saline (PBS) and 10% fetal bovine serum (FBS) and cryopreserved at −80°C in 50% FBS, 40% RPMI 1640, and 10% dimethyl sulfoxide.

scRNA-seq and scTCR-seq libraries
Thawed PBMCs (*n* = 2) and CBMCs (*n* = 2) were cultured overnight in X-Vivo 15 medium (Lonza, Basel, Switzerland), and live γδ T cells were sorted on an Aria Fusion cytometer (BD Biosciences). Libraries for single-cell transcriptome sequencing and scTCR-seq were prepared using the Chromium Single-Cell 5′ Library Gel Bead and Construction Kit and Chromium Single-Cell V(D)J Enrichment Kit (10x Genomics, CA, USA). Custom primers were used for the enrichment of γδ TCR transcripts. Primer sequences and details on library preparation are described in Supplementary Methods. Agilent Bioanalyzer high-sensitivity chips were applied for quality control of scRNA-seq and scTCR-seq libraries. The scRNA-seq libraries were sequenced on the Illumina NextSeq 500/550 platform, and scTCR-seq libraries were sequenced on the Illumina MiSeq or the Illumina NextSeq 500/550 platform.

Data processing of scRNA-seq libraries
The scRNA-seq reads were aligned to the human reference genome GRCh38 (UCSC, CA, USA), after generation of cell-gene matrices via Cell Ranger v3.1 (10x Genomics). Data from ambient RNA were filtered on the basis of UMI-barcode saturation curve.

Cell clustering and DEG profile
The R package Seurat v3.1 was used under R v3.6.3 for scRNA-seq data dimensional reduction, cell clustering, and differential expression analysis (*66, 67*). Mitochondria, ribosomal, and cycling gene content were regressed out as unwanted variance (*68*), and GSEA was performed and visualized by the R package clusterProfiler (*69*). Immunological gene sets from the Molecular Signatures Database (Broad Institute, MA, USA) were used as reference datasets. A more detailed description is provided in Supplementary Methods.

Identification of GMs
The top 100 up-regulated DEGs of each cluster were used for the identification of GMs. Mitochondrial, ribosomal, and TCR genes were removed. The average gene expression values per cluster were calculated from normalized single-cell expression values, and the gene-to-cluster matrix was then log-transformed and scaled on gene level. Next, this average gene expression matrix was subjected to UMAP embedding. GMs were identified by hierarchical clustering method under "average" model (height cutoff = 3). Clusters with similar expression patterns were merged as one GM. Gene Ontology (biological process) enrichment analysis was performed on GMs by the R package clusterProfiler. Aggregated GM expression scores were calculated on single-cell base by "AddModuleScore" function from Seurat.

scTCR-seq analysis

Cell Ranger VDJ tools v3.1 (10x Genomics) was performed to generate scTCR annotations. Human genome GRCh38 was used as the reference for alignment. The annotated scTCR-seq data from multiple sequencing runs from the same sample were merged. Nonproductive TCR sequences and duplicates were excluded. Further, by matching the barcodes, scTCR-seq data were incorporated into the metadata of scRNA-seq Seurat project. Gini indices of paired TCR clones were calculated by R package reldist.

Public *TRD* clones were defined on the basis of comparison of single-cell *TRD* repertoires from 4 donors in this study and bulk *TRD* repertoires from 80 donors (*11, 18, 36, 70*). Among them were 21 adults and 63 children aged between 0 and 3.5 years. CDR3 regions were used for comparison. *TRD* clones were defined as public if their CDR3 sequence was recovered from at least two donors.

Bulk TCR-seq analysis

Bulk *TRD* repertoires of the respective subsets were generated from FACS-sorted cells of fresh PBMCs ($n = 4$). Antibodies used and gating strategies in this experiment are specified in Supplementary Methods. RNA isolation (Qiagen, Hilden, Germany) and cDNA synthesis (SuperScript III, Invitrogen, CA, USA) were performed after cell lysis. Next, CDR3 regions of *TRD* were amplified via gene-specific primers as previously described (*11*). Libraries were sequenced (paired-end, 500 cycles) on the Illumina MiSeq platform. Annotation of fastq files was performed according to the International Immunogenetics Information System (IMGT) using MiXCR software (*71*). Annotated read files were summarized using VDJTools (*72*).

Single-cell transcriptome analysis of fetal thymocytes

Ewk8 to Ewk10 thymocyte expression matrices were acquired from GEO: GSE133341. Cell identity was assigned by the expression of TCR genes. GM scores were calculated on the basis of GMs identified in our PB and CB datasets.

Multicolor flow cytometry and functional assays

Flow cytometry was performed using an LSR II cytometer (BD Biosciences) or a Cytek Aurora spectral flow cytometer (Cytek Biosciences), and data were analyzed by FlowJo v10 software (Tree Star) and R 3.6.3. Antibodies and a more detailed description of functional assays can be found in Supplementary Methods. For multicolor flow cytometry using nine surface markers established by transcriptome analysis, cell suspensions of thawed PBMCs ($n = 6$) or CBMCs ($n = 5$) (2×10^6 cells) were treated with 5% Fc receptor block in buffer (PBS with 3% fetal calf serum and 4 mM EDTA) before staining. Intracellular staining was performed with the Foxp3/TF Staining Buffer Set (eBioscience) and antibodies for RORγt and T-bet. Acquisition was performed on a Cytek Aurora cytometer. For 12-day "T$_H$17-polarizing" cultures, fresh CBMCs were isolated and stimulated with a cytokine cocktail [10 ng/ml of each IL-1β, IL-23, and TGFβ (all Peprotech) as well as IL-6 (50 ng/ml; R&D Systems)] and 10 μM isopentenyl pyrophosphate (Sigma-Aldrich). On day 6, IL-2 was added at 20 U/ml, and on day 12, cells were restimulated with phorbol 12-myristate 13-acetate (PMA)/ionomycin (Sigma-Aldrich, Invitrogen) before intracellular cytokine staining (BD Cytofix/Cytoperm Kit). Cells were subsequently analyzed by flow cytometry. In some experiments, live CD3$^+$ TCR γδ$^+$ TCR Vδ2$^+$ T cells from CBMCs were sorted into two populations: CD94$^-$ CCR6$^+$CD26$^+$ and CCR6$^-$ Vδ2 T cells. Both populations were cultured for 12 days, and 2×10^5 irradiated (30-gray) autologous CBMCs were added to each well.

Differences in IFN-γ and TNFα expression on Vδ1 T cells were studied using PBMCs ($n = 10$) stimulated for 3 hours with PMA/ionomycin and brefeldin A (Sigma-Aldrich). After stimulation, cells were stained for extracellular markers, and intracellular IFN-γ and TNFα staining was performed with the Cytofix/Cytoperm Kit (BD Biosciences). Acquisition was performed on a Cytek Aurora cytometer. Analysis of patients with SCID and controls was performed with whole blood of healthy controls ($n = 21$) and patients with SCID ($n = 3$) and was analyzed as previously described (*73*). Briefly, 500 μl of whole blood was processed in erythrocyte lysis buffer. Samples were stained for 20 min in PBS at room temperature, washed twice, and acquired on a Cytek Aurora spectral flow cytometer.

Multicolor flow cytometry data analysis

Flow cytometry (FACS) data were analyzed on the basis of the CyTOF workflow (*74*). Briefly, TCRγδ$^+$ subsets from PBMC and CBMC were gated and isolated by FlowJo software (BD Biosciences) and exported to R v3.6.3. Biexponential transformation was applied to raw fluorescent intensities allowing to remove background fluorescence and spreading error (*75*). Scaled expression values were subjected for unsupervised clustering and UMAP embedding. Unsupervised clustering was conducted with R package FlowSOM (*76*) and ConsensusClusterPlus (*77*).

Statistical analysis

The statistical tests that were used in each experiment are specified in each figure legend. Data were analyzed with R 3.6.3.

SUPPLEMENTARY MATERIALS

immunology.sciencemag.org/cgi/content/full/6/58/eabf0125/DC1
Methods
Fig. S1. Isolation of human γδ T cells for single-cell NGS.
Fig. S2. Quality control and overview of scRNA-seq data.
Fig. S3. Overview of scTCR-seq data.
Fig. S4. Vγ9Vδ2 γδ T cells are innate T cells with constitutive TCR.
Fig. S5. FACS identification of type 3 Vδ2$^+$ cells.
Fig. S6. Type 3 γδ T cells show distinct TCR repertoire profiles.
Fig. S7. TCR expression of fetal thymocytes.
Fig. S8. Vδ1$^+$ γδ CTLs mature into PD1^{hi} and PD1^{low} cells.
Fig. S9. Differentially expressed surface protein genes.
Fig. S10. Multicolor FACS reproduces the heterogeneity revealed by scRNA-seq.
Table S1. Gene coexpression modules.

View/request a protocol for this paper from *Bio-protocol*.

REFERENCES AND NOTES

1. Z. Sebestyen, I. Prinz, J. Déchanet-Merville, B. Silva-Santos, J. Kuball, Translating gammadelta (γδ) T cells and their receptors into cancer cell therapies. *Nat. Rev. Drug Discov.* **19**, 169–184 (2020).
2. P. Vantourout, A. Hayday, Six-of-the-best: Unique contributions of γδ T cells to immunology. *Nat. Rev. Immunol.* **13**, 88–100 (2013).
3. A. S. Fichtner, S. Ravens, I. Prinz, Human γδ TCR repertoires in health and disease. *Cells* **9**, 800 (2020).
4. P. Constant, F. Davodeau, M. A. Peyrat, Y. Poquet, G. Puzo, M. Bonneville, J. J. Fournie, Stimulation of human gamma delta T cells by nonpeptidic mycobacterial ligands. *Science* **264**, 267–270 (1994).
5. F. Halary, V. Pitard, D. Dlubek, R. Krzysiek, H. de la Salle, P. Merville, C. Dromer, D. Emilie, J. F. Moreau, J. Déchanet-Merville, Shared reactivity of Vδ2^{neg} γδ T cells against cytomegalovirus-infected cells and tumor intestinal epithelial cells. *J. Exp. Med.* **201**, 1567–1578 (2005).
6. M. M. Karunakaran, C. R. Willcox, M. Salim, D. Paletta, A. S. Fichtner, A. Noll, L. Starick, A. Nöhren, C. R. Begley, K. A. Berwick, R. A. G. Chaleil, V. Pitard, J. Déchanet-Merville, P. A. Bates, B. Kimmel, T. J. Knowles, V. Kunzmann, L. Walter, M. Jeeves, F. Mohammed,

B. E. Willcox, T. Herrmann, Butyrophilin-2A1 directly binds germline-encoded regions of the Vγ9Vδ2 TCR and is essential for phosphoantigen sensing. *Immunity* **52**, 487–498.e6 (2020).

7. M. Rigau, S. Ostrouska, T. S. Fulford, D. N. Johnson, K. Woods, Z. Ruan, H. E. G. McWilliam, C. Hudson, C. Tutuka, A. K. Wheatley, S. J. Kent, J. A. Villadangos, B. Pal, C. Kurts, J. Simmonds, M. Pelzing, A. D. Nash, A. Hammet, A. M. Verhagen, G. Vairo, E. Maraskovsky, C. Panousis, N. A. Gherardin, J. Cebon, D. I. Godfrey, A. Behren, A. P. Uldrich, Butyrophilin 2A1 is essential for phosphoantigen reactivity by γδ T cells. *Science* **367**, eaay5516 (2020).

8. Y. Xu, Z. Xiang, M. Alnaggar, L. Kouakanou, J. Li, J. He, J. Yang, Y. Hu, Y. Chen, L. Lin, J. Hao, J. Li, J. Chen, M. Li, Q. Wu, C. Peters, Q. Zhou, J. Li, Y. Liang, X. Wang, B. Han, M. Ma, D. Kabelitz, K. Xu, W. Tu, Y. Wu, Z. Yin, Allogeneic Vγ9Vδ2 T-cell immunotherapy exhibits promising clinical safety and prolongs the survival of patients with late-stage lung or liver cancer. *Cell. Mol. Immunol.* **18**, 427–439 (2020).

9. N. M. Provine, B. Binder, M. E. B. FitzPatrick, A. Schuch, L. C. Garner, K. D. Williamson, B. van Wilgenburg, R. Thimme, P. Klenerman, M. Hofmann, Unique and common features of innate-like human Vδ2+ γδT cells and mucosal-associated invariant T cells. *Front. Immunol.* **9**, 756 (2018).

10. K. M. Wragg, H.-X. Tan, A. B. Kristensen, C. V. Nguyen-Robertson, A. D. Kelleher, M. S. Parsons, A. K. Wheatley, S. P. Berzins, D. G. Pellicci, S. J. Kent, J. A. Juno, High CD26 and low CD94 expression identifies an IL-23 responsive Vδ2+ T cell subset with a MAIT cell-like transcriptional profile. *Cell Rep.* **31**, 107773 (2020).

11. S. Ravens, C. Schultze-Florey, S. Raha, I. Sandrock, M. Drenker, L. Oberdörfer, A. Reinhardt, I. Ravens, M. Beck, R. Geffers, C. Von Kaisenberg, M. Heuser, F. Thol, A. Ganser, R. Förster, C. Koenecke, I. Prinz, Human γδ T cells are quickly reconstituted after stem-cell transplantation and show adaptive clonal expansion in response to viral infection. *Nat. Immunol.* **18**, 393–401 (2017).

12. M. S. Davey, C. R. Willcox, S. P. Joyce, K. Ladell, S. A. Kasatskaya, J. E. McLaren, S. Hunter, M. Salim, F. Mohammed, D. A. Price, D. M. Chudakov, B. E. Willcox, Clonal selection in the human Vδ1 T cell repertoire indicates γδ TCR-dependent adaptive immune surveillance. *Nat. Commun.* **8**, 14760 (2017).

13. I. Prinz, B. Silva-Santos, D. J. D. J. Pennington, Functional development of γδ T cells. *Eur. J. Immunol.* **43**, 1988–1994 (2013).

14. J. D. Haas, S. Ravens, S. Düber, I. Sandrock, L. Oberdörfer, E. Kashani, V. Chennupati, L. Föhse, R. Naumann, S. Weiss, A. Krueger, R. Förster, I. Prinz, Development of interleukin-17-producing γδ T cells is restricted to a functional embryonic wave. *Immunity* **37**, 48–59 (2012).

15. L. Tan, I. Sandrock, I. Odak, Y. Aizenbud, A. Wilharm, J. Barros-Martins, Y. Tabib, A. Borchers, T. Amado, L. Gangoda, M. J. Herold, M. Schmidt-Supprian, J. Kisielow, B. Silva-Santos, C. Koenecke, A.-H. Hovav, C. Krebs, I. Prinz, S. Ravens, Single-cell transcriptomics identifies the adaptation of Scart1+ Vγ6+ T cells to skin residency as activated effector cells. *Cell Rep.* **27**, 3657–3671.e4 (2019).

16. L. D. McVay, S. R. Carding, Extrathymic origin of human gamma delta T cells during fetal development. *J. Immunol.* **157**, 2873–2882 (1996).

17. T. Dimova, M. Brouwer, F. Gosselin, J. Tassignon, O. Leo, C. Donner, A. Marchant, D. Vermijlen, Effector Vγ9Vδ2 T cells dominate the human fetal γδ T-cell repertoire. *Proc. Natl. Acad. Sci. U.S.A.* **112**, E556–E565 (2015).

18. A. S. Fichtner, A. Bubke, F. Rampoldi, A. Wilharm, L. Tan, L. Steinbrück, C. Schultze-Florey, C. Kaisenberg, I. Prinz, T. Herrmann, S. Ravens, TCR repertoire analysis reveals phosphoantigen-induced polyclonal proliferation of Vγ9Vδ2 T cells in neonates and adults. *J. Leukoc. Biol.* **107**, 1023–1032 (2020).

19. D. Vermijlen, I. Prinz, Ontogeny of innate T lymphocytes - some innate lymphocytes are more innate than others. *Front. Immunol.* **5**, 486 (2014).

20. B. Di Lorenzo, S. Ravens, B. Silva-Santos, High-throughput analysis of the human thymic Vδ1+ T cell receptor repertoire. *Sci. data.* **6**, 115 (2019).

21. J. C. Ribot, S. T. Ribeiro, D. V. Correia, A. E. Sousa, B. Silva-Santos, Human γδ thymocytes are functionally immature and differentiate into cytotoxic type 1 effector T cells upon IL-2/IL-15 signaling. *J. Immunol.* **192**, 2237–2243 (2014).

22. P. Tieppo, M. Papadopoulou, D. Gatti, N. McGovern, J. K. K. Y. Chan, F. Gosselin, G. Goetgeluk, K. Weening, L. Ma, N. Dauby, A. Cogan, C. Donner, F. Ginhoux, B. Vandekerckhove, D. Vermijlen, The human fetal thymus generates invariant effector γδ T cells. *J. Exp. Med.* **217**, jem.20190580 (2019).

23. G. Pizzolato, H. Kaminski, M. Tosolini, D.-M. Franchini, F. Pont, F. Martins, C. Valle, D. Labourdette, S. Cadot, A. Quillet-Mary, M. Poupot, C. Laurent, L. Ysebaert, S. Meraviglia, F. Dieli, P. Merville, P. Milpied, J. Déchanet-Merville, J.-J. Fournié, Single-cell RNA sequencing unveils the shared and the distinct cytotoxic hallmarks of human TCRVδ1 and TCRVδ2 γδ T lymphocytes. *Proc. Natl. Acad. Sci. U.S.A.* **116**, 11906–11915 (2019).

24. M. S. Davey, C. R. Willcox, S. Hunter, S. A. Kasatskaya, E. B. M. Remmerswaal, M. Salim, F. Mohammed, F. J. Bemelman, D. M. Chudakov, Y. H. Oo, B. E. Willcox, The human Vδ2+ T-cell compartment comprises distinct innate-like Vγ9+ and adaptive Vγ9- subsets. *Nat. Commun.* **9**, 1760 (2018).

25. S. Xing, F. Li, Z. Zeng, Y. Zhao, S. Yu, Q. Shan, Y. Li, F. C. Phillips, P. K. Maina, H. H. Qi, C. Liu, J. Zhu, R. M. Pope, C. A. Musselman, C. Zeng, W. Peng, H.-H. Xue, Tcf1 and Lef1 transcription factors establish CD8+ T cell identity through intrinsic HDAC activity. *Nat. Immunol.* **17**, 695–703 (2016).

26. P. A. Szabo, H. M. Levitin, M. Miron, M. E. Snyder, T. Senda, J. Yuan, Y. L. Cheng, E. C. Bush, P. Dogra, P. Thapa, D. L. Farber, P. A. Sims, Single-cell transcriptomics of human T cells reveals tissue and activation signatures in health and disease. *Nat. Commun.* **10**, 4706 (2019).

27. Sagar, M. Pokrovskii, J. S. Herman, S. Naik, E. Sock, P. Zeis, U. Lausch, M. Wegner, Y. Tanriver, D. R. Littman, D. Grün, Deciphering the regulatory landscape of fetal and adult γδ T-cell development at single-cell resolution. *EMBO J.* **39**, e104159 (2020).

28. S. Gérart, S. Sibéril, E. Martin, C. Lenoir, C. Aguilar, C. Picard, O. Lantz, A. Fischer, S. Latour, Human iNKT and MAIT cells exhibit a PLZF-dependent proapoptotic propensity that is counterbalanced by XIAP. *Blood* **121**, 614–623 (2013).

29. K. Narayan, K. E. Sylvia, N. Malhotra, C. C. Yin, G. Martens, T. Vallerskog, H. Kornfeld, N. Xiong, N. R. Cohen, M. B. Brenner, L. J. Berg, K. Kang; The Immunological Genome Project Consortium, Intrathymic programming of effector fates in three molecularly distinct γδ T cell subtypes. *Nat. Immunol.* **13**, 511–518 (2012).

30. K. Venken, P. Jacques, C. Mortier, M. E. Labadia, T. Decruy, J. Coudenys, K. Hoyt, A. L. Wayne, R. Hughes, M. Turner, S. Van Gassen, L. Martens, D. Smith, C. Harcken, J. Wahle, C. T. Wang, E. Verheugen, N. Schryvers, G. Varkas, H. Cypers, R. Wittoek, Y. Piette, L. Gyselbrecht, S. Van Calenbergh, F. Van den Bosch, Y. Saeys, G. Nabozny, D. Elewaut, RORγt inhibition selectively targets IL-17 producing iNKT and γδ-T cells enriched in Spondyloarthritis patients. *Nat. Commun.* **10**, 9 (2019).

31. N. A. Spidale, K. Sylvia, K. Narayan, B. Miu, M. Frascoli, H. J. Melichar, W. Zhihao, J. Kisielow, A. Palin, T. Serwold, P. Love, M. Kobayashi, M. Yoshimoto, N. Jain, J. Kang, Interleukin-17-producing γδ T cells originate from SOX13+ progenitors that are independent of γδTCR signaling. *Immunity* **49**, 857–872.e5 (2018).

32. Y. Lu, X. Cao, X. Zhang, D. Kovalovsky, PLZF controls the development of fetal-derived IL-17+ Vγ6+ γδ T cells. *J. Immunol.* **195**, 4273–4281 (2015).

33. C. R. Willcox, M. S. Davey, B. E. Willcox, Development and selection of the human Vγ9Vδ2+ T-cell repertoire. *Front. Immunol.* **9**, 1501 (2018).

34. M. Papadopoulou, P. Tieppo, N. McGovern, F. Gosselin, J. K. Y. Chan, G. Goetgeluk, N. Dauby, A. Cogan, C. Donner, F. Ginhoux, B. Vandekerckhove, D. Vermijlen, TCR sequencing reveals the distinct development of fetal and adult human Vγ9Vδ2 T cells. *J. Immunol.* **203**, 1468–1479 (2019).

35. A. M. Sherwood, C. Desmarais, R. J. Livingston, J. Andriesen, M. Haussler, C. S. Carlson, H. Robins, Deep sequencing of the human TCR and TCR repertoires suggests that TCR rearranges after and T cell commitment. *Sci. Transl. Med.* **3**, 90ra61 (2011).

36. S. Ravens, A. S. Fichtner, M. Willers, D. Torkornoo, S. Pirr, J. Schöning, M. Deseke, I. Sandrock, A. Bubke, A. Wilharm, D. Dodoo, B. Egyir, K. L. Flanagan, L. Steinbrück, P. Dickinson, P. Ghazal, B. Adu, D. Viemann, I. Prinz, Microbial exposure drives polyclonal expansion of innate γδ T cells immediately after birth. *Proc. Natl. Acad. Sci. U.S.A.* **117**, 18649–18660 (2020).

37. M. Papadopoulou, T. Dimova, M. Shey, L. Briel, H. Veldtsman, N. Khomba, H. Africa, M. Steyn, W. A. Hanekom, T. J. Scriba, E. Nemes, D. Vermijlen, Fetal public Vγ9Vδ2 T cells expand and gain potent cytotoxic functions early after birth. *Proc. Natl. Acad. Sci. U.S.A.* **117**, 18638–18648 (2020).

38. I. Engel, G. Seumois, L. Chavez, D. Samaniego-Castruita, B. White, A. Chawla, D. Mock, P. Vijayanand, M. Kronenberg, Innate-like functions of natural killer T cell subsets result from highly divergent gene programs. *Nat. Immunol.* **17**, 728–739 (2016).

39. E. Moens, M. Brouwer, T. Dimova, M. Goldman, F. Willems, D. Vermijlen, IL-23R and TCR signaling drives the generation of neonatal Vγ9Vδ2 T cells expressing high levels of cytotoxic mediators and producing IFN-γ and IL-17. *J. Leukoc. Biol.* **89**, 743–752 (2011).

40. K. J. Ness-Schwickerath, C. Jin, C. T. Morita, Cytokine requirements for the differentiation and expansion of IL-17A– and IL-22–producing human Vγ2Vδ2 T cells. *J. Immunol.* **184**, 7268–7280 (2010).

41. N. Caccamo, C. La Mendola, V. Orlando, S. Meraviglia, M. Todaro, G. Stassi, G. Sireci, J. J. Fournié, F. Dieli, Differentiation, phenotype, and function of interleukin-17-producing human vγ9vδ2 T cells. *Blood* **118**, 129–138 (2011).

42. R. L. O'Brien, W. K. Born, Two functionally distinct subsets of IL-17 producing γδ T cells. *Immunol. Rev.* **298**, 10–24 (2020).

43. Y. Zeng, C. Liu, Y. Gong, Z. Bai, S. Hou, J. He, Z. Bian, Z. Li, Y. Ni, J. Yan, T. Huang, H. Shi, C. Ma, X. Chen, J. Wang, L. Bian, Y. Lan, B. Liu, H. Hu, Single-cell RNA sequencing resolves spatiotemporal development of pre-thymic lymphoid progenitors and thymus organogenesis in human embryos. *Immunity* **51**, 930–948.e6 (2019).

44. A. Reinhardt, S. Ravens, H. Fleige, J. D. Haas, L. Oberdörfer, M. Łyszkiewicz, R. Förster, I. Prinz, CCR7-mediated migration in the thymus controls γδ T-cell development. *Eur. J. Immunol.* **44**, 1320–1329 (2014).

45. C. Liu, F. Saito, Z. Liu, Y. Lei, S. Uehara, P. Love, M. Lipp, S. Kondo, N. Manley, Y. Takahama, Coordination between CCR7- and CCR9-mediated chemokine signals in prevascular fetal thymus colonization. *Blood* **108**, 2531–2539 (2006).

46. J.-E. Park, R. A. Botting, C. Domínguez Conde, D.-M. Popescu, M. Lavaert, D. J. Kunz, I. Goh, E. Stephenson, R. Ragazzini, E. Tuck, A. Wilbrey-Clark, K. Roberts, V. R. Kedlian, J. R. Ferdinand, X. He, S. Webb, D. Maunder, N. Vandamme, K. T. Mahbubani, K. Polanski, L. Mamanova, L. Bolt, D. Crossland, F. de Rita, A. Fuller, A. Filby, G. Reynolds, D. Dixon, K. Saeb-Parsy, S. Lisgo, D. Henderson, R. Vento-Tormo, O. A. Bayraktar, R. A. Barker, K. B. Meyer, Y. Saeys, P. Bonfanti, S. Behjati, M. R. Clatworthy, T. Taghon, M. Haniffa, S. A. Teichmann, A cell atlas of human thymic development defines T cell repertoire formation. *Science* **367**, eaay3224 (2020).

47. J. Duraiswamy, C. C. Ibegbu, D. Masopust, J. D. Miller, K. Araki, G. H. Doho, P. Tata, S. Gupta, M. J. Zilliox, H. I. Nakaya, B. Pulendran, W. N. Haining, G. J. Freeman, R. Ahmed, Phenotype, function, and gene expression profiles of programmed death-1hi CD8 T cells in healthy human adults. *J. Immunol.* **186**, 4200–4212 (2011).

48. B. Bengsch, B. Seigel, T. Flecken, J. Wolanski, H. E. Blum, R. Thimme, Human Th17 cells express high levels of enzymatically active dipeptidylpeptidase IV (CD26). *J. Immunol.* **188**, 5438–5447 (2012).

49. P. L. Ryan, N. Sumaria, C. J. Holland, C. M. Bradford, N. Izotova, C. L. Grandjean, A. S. Jawad, L. A. Bergmeier, D. J. Pennington, Heterogeneous yet stable Vδ2(+) T-cell profiles define distinct cytotoxic effector potentials in healthy human individuals. *Proc. Natl. Acad. Sci. U.S.A.* **113**, 14378–14383 (2016).

50. N. Caccamo, S. Meraviglia, V. Ferlazzo, D. Angelini, G. Borsellino, F. Poccia, L. Battistini, F. Dieli, A. Salerno, Differential requirements for antigen or homeostatic cytokines for proliferation and differentiation of human Vγ9Vδ2 naive, memory and effector T cell subsets. *Eur. J. Immunol.* **35**, 1764–1772 (2005).

51. E. Bruni, V. Cazzetta, M. Donadon, M. Cimino, G. Torzilli, G. Spata, G. Leonardi, F. Dieli, J. Mikulak, D. Mavilio, Chemotherapy accelerates immune-senescence and functional impairments of Vδ2pos T cells in elderly patients affected by liver metastatic colorectal cancer. *J. Immunother. Cancer* **7**, 347 (2019).

52. M. Heiden, S. Björkander, K. Rahman Qazi, J. Bittmann, L. Hell, M. C. Jenmalm, G. Marchini, D. Vermijlen, T. Abrahamsson, C. Nilsson, E. Sverremark-Ekström, Characterization of the γδ T-cell compartment during infancy reveals clear differences between the early neonatal period and 2 years of age. *Immunol. Cell Biol.* **98**, 79–87 (2020).

53. M. J. Kallemeijn, F. G. Kavelaars, M. Y. van der Klift, I. L. M. Wolvers-Tettero, P. J. M. Valk, J. J. M. van Dongen, A. W. Langerak, Next-generation sequencing analysis of the human TCRγδ+ T-cell repertoire reveals shifts in Vγ- and Vδ-usage in memory populations upon aging. *Front. Immunol.* **9**, 448 (2018).

54. Y. J. Lee, G. J. Starrett, S. T. Lee, R. Yang, C. M. Henzler, S. C. Jameson, K. A. Hogquist, Lineage-specific effector signatures of invariant NKT cells are shared amongst γδ T, innate lymphoid, and Th cells. *J. Immunol.* **197**, 1460–1470 (2016).

55. T. Kreslavsky, A. K. Savage, R. Hobbs, F. Gounari, R. Bronson, P. Pereira, P. P. Pandolfi, A. Bendelac, H. Von Boehmer, TCR-inducible PLZF transcription factor required for innate phenotype of a subset of γδ T cells with restricted TCR diversity. *Proc. Natl. Acad. Sci. U.S.A.* **106**, 12453–12458 (2009).

56. M. G. Constantinides, H. Gudjonson, B. D. McDonald, I. E. Ishizuka, P. A. Verhoef, A. R. Dinner, A. Bendelac, PLZF expression maps the early stages of ILC1 lineage development. *Proc. Natl. Acad. Sci. U.S.A.* **112**, 5123–5128 (2015).

57. M. Lee, E. Lee, S. K. Han, Y. H. Choi, D.-i. Kwon, H. Choi, K. Lee, E. S. Park, M. S. Rha, D. J. Joo, E. C. Shin, S. Kim, J. K. Kim, Y. J. Lee, Single-cell RNA sequencing identifies shared differentiation paths of mouse thymic innate T cells. *Nat. Commun.* **11**, 4367 (2020).

58. J. C. Ribot, A. deBarros, D. J. Pang, J. F. Neves, V. Peperzak, S. J. Roberts, M. Girardi, J. Borst, A. C. Hayday, D. J. Pennington, B. Silva-Santos, CD27 is a thymic determinant of the balance between interferon-γ- and interleukin 17–producing γδ T cell subsets. *Nat. Immunol.* **10**, 427–436 (2009).

59. T. Cupedo, N. K. Crellin, N. Papazian, E. J. Rombouts, K. Weijer, J. L. Grogan, W. E. Fibbe, J. J. Cornelissen, H. Spits, Human fetal lymphoid tissue–inducer cells are interleukin 17–producing precursors to RORC+ CD127+ natural killer–like cells. *Nat. Immunol.* **10**, 66–74 (2009).

60. L. Maggi, V. Santarlasci, M. Capone, A. Peired, F. Frosali, S. Q. Crome, V. Querci, M. Fambrini, F. Liotta, M. K. Levings, E. Maggi, L. Cosmi, S. Romagnani, F. Annunziato, CD161 is a marker of all human IL-17-producing T-cell subsets and is induced by RORC. *Eur. J. Immunol.* **40**, 2174–2181 (2010).

61. S. P. Singh, H. H. Zhang, J. F. Foley, M. N. Hedrick, J. M. Farber, Human T cells that are able to produce IL-17 express the chemokine receptor CCR6. *J. Immunol.* **180**, 214–221 (2008).

62. U. Laggner, P. Di Meglio, G. K. Perera, C. Hundhausen, K. E. Lacy, N. Ali, C. H. Smith, A. C. Hayday, B. J. Nickoloff, F. O. Nestle, Identification of a novel proinflammatory human skin-homing Vγ9Vδ2 T cell subset with a potential role in psoriasis. *J. Immunol.* **187**, 2783–2793 (2011).

63. M.-L. Michel, D. J. Pang, S. F. Y. Haque, A. J. Potocnik, D. J. Pennington, A. C. Hayday, Interleukin 7 (IL-7) selectively promotes mouse and human IL-17–producing cells. *Proc. Natl. Acad. Sci. U.S.A.* **109**, 17549–17554 (2012).

64. C. Kessel, K. Lippitz, T. Weinhage, C. Hinze, H. Wittkowski, D. Holzinger, N. Fall, A. A. Grom, N. Gruen, D. Foell, Proinflammatory cytokine environments can drive interleukin-17

65. overexpression by γ/δ T cells in systemic juvenile idiopathic arthritis. *Arthritis Rheumatol.* **69**, 1480–1494 (2017).

65. J. D. Haas, F. H. M. González, S. Schmitz, V. Chennupati, L. Föhse, E. Kremmer, R. Förster, I. Prinz, CCR6 and NK1.1 distinguish between IL-17A and IFN-γ-producing γδ effector T cells. *Eur. J. Immunol.* **39**, 3488–3497 (2009).

66. T. Stuart, A. Butler, P. Hoffman, C. Hafemeister, E. Papalexi, W. M. Mauck III, Y. Hao, M. Stoeckius, P. Smibert, R. Satija, Comprehensive integration of single-cell data. *Cell* **177**, 1888–1902.e21 (2019).

67. A. Butler, P. Hoffman, P. Smibert, E. Papalexi, R. Satija, Integrating single-cell transcriptomic data across different conditions, technologies, and species. *Nat. Biotechnol.* **36**, 411–420 (2018).

68. M. S. Kowalczyk, I. Tirosh, D. Heckl, T. N. Rao, A. Dixit, B. J. Haas, R. K. Schneider, A. J. Wagers, B. L. Ebert, A. Regev, Single-cell RNA-seq reveals changes in cell cycle and differentiation programs upon aging of hematopoietic stem cells. *Genome Res.* **25**, 1860–1872 (2015).

69. G. Yu, L.-G. Wang, Y. Han, Q.-Y. He, clusterProfiler: An R package for comparing biological themes among gene clusters. *OMICS* **16**, 284–287 (2012).

70. S. Ravens, J. Hengst, V. Schlapphoff, K. Deterding, A. Dhingra, C. Schultze-Florey, C. Koenecke, M. Cornberg, H. Wedemeyer, I. Prinz, Human γδ T cell receptor repertoires in peripheral blood remain stable despite clearance of persistent hepatitis C virus infection by direct-acting antiviral drug therapy. *Front. Immunol.* **9**, 510 (2018).

71. D. A. Bolotin, S. Poslavsky, I. Mitrophanov, M. Shugay, I. Z. Mamedov, E. V. Putintseva, D. M. Chudakov, MiXCR: Software for comprehensive adaptive immunity profiling. *Nat. Methods* **12**, 380–381 (2015).

72. M. Shugay, D. V. Bagaev, M. A. Turchaninova, D. A. Bolotin, O. V. Britanova, E. V. Putintseva, M. V. Pogorelyy, V. I. Nazarov, I. V. Zvyagin, V. I. Kirgizova, K. I. Kirgizov, E. V. Skorobogatova, D. M. Chudakov, VDJtools: Unifying post-analysis of T cell receptor repertoires. *PLOS Comput. Biol.* **11**, e1004503 (2015).

73. I. Odak, J. Barros-Martins, B. Bošnjak, K. Stahl, S. David, O. Wiesner, M. Busch, M. M. Hoeper, I. Pink, T. Welte, M. Cornberg, M. Stoll, L. Goudeva, R. Blasczyk, A. Ganser, I. Prinz, R. Förster, C. Koenecke, C. R. Schultze-Florey, Reappearance of effector T cells is associated with recovery from COVID-19. *EBioMedicine* **57**, 102885 (2020).

74. M. Nowicka, C. Krieg, L. M. Weber, F. J. Hartmann, S. Guglietta, B. Becker, M. P. Levesque, M. D. Robinson, CyTOF workflow: Differential discovery in high-throughput high-dimensional cytometry datasets. *F1000Res.* **6**, 748 (2017).

75. E. M. C. Mazza, J. Brummelman, G. Alvisi, A. Roberto, F. De Paoli, V. Zanon, F. Colombo, M. Roederer, E. Lugli, Background fluorescence and spreading error are major contributors of variability in high-dimensional flow cytometry data visualization by t-distributed stochastic neighboring embedding. *Cytometry A.* **93**, 785–792 (2018).

76. S. Van Gassen, B. Callebaut, M. J. Van Helden, B. N. Lambrecht, P. Demeester, T. Dhaene, Y. Saeys, FlowSOM: Using self-organizing maps for visualization and interpretation of cytometry data. *Cytometry A.* **87**, 636–645 (2015).

77. M. D. Wilkerson, D. N. Hayes, ConsensusClusterPlus: A class discovery tool with confidence assessments and item tracking. *Bioinformatics* **26**, 1572–1573 (2010).

Science Immunology

A fetal wave of human type 3 effector ## cells with restricted TCR diversity persists into adulthood

Likai TanAlina Suzann FichtnerElena BruniIvan OdakInga SandrockAnja BubkeAlina BorchersChristian Schultze-FloreyChristian KoeneckeReinhold FörsterMichael JarekConstantin von KaisenbergAnsgar SchulzXiaojing ChuBowen ZhangYang LiUlf PanzerChristian F. KrebsSarina RavensImmo Prinz

Early emergence

T cells are an innate-like subset of T cells that can recognize and respond to microbes. Tan *et al.* studied the activation and differentiation of ## T cells to better understand the development and persistence of these cells. They used single-cell RNA sequencing and paired ##TCR analysis from neonatal cord blood or adult peripheral blood and observed a high level of heterogeneity that correlated with TCR usage in immature and differentiated ## T cell clusters. They detected type 1– and type 3–like V#9V#2 T cell subsets with distinct sets of TCR clonotypes, and similar type 3 V#9V#2 T cells were found in neonatal cord blood and the early fetal thymus, suggesting that these cells emerge early in fetal development and can persist into adulthood.

View the article online
https://www.science.org/doi/10.1126/sciimmunol.abf0125
Permissions
https://www.science.org/help/reprints-and-permissions

Use of think article is subject to the Terms of service